https://doi.org/10.5194/egusphere-2023-2583
Preprint. Discussion started: 27 November 2023

Oceanic gateways to Antarctic grounding lines – Impact of critical access depths on sub-shelf melt

Lena Nicola[1,2], Ronja Reese[1,3], Moritz Kreuzer[1,2], Torsten Albrecht[1], and Ricarda Winkelmann[1,2]

[1] Potsdam Institute for Climate Impact Research (PIK), Member of the Leibniz Association, P.O. Box 60 12 03, D-14412 Potsdam, Germany
[2] Institute of Physics and Astronomy, University of Potsdam, Karl-Liebknecht-Str. 24-25, 14476 Potsdam, Germany
[3] Department of Geography and Environmental Sciences, Northumbria University, Newcastle, UK

Correspondence: Lena Nicola (lena.nicola@pik-potsdam.de) and Ricarda Winkelmann (ricarda.winkelmann@pik-potsdam.de)

Abstract. Melting underneath the floating ice shelves surrounding the Antarctic continent is a key process for the stability of the Antarctic Ice Sheet and therefore its current and future mass loss. Troughs and sills on the continental shelf play a crucial role in modulating sub-shelf melt rates, as they can allow or block the access of relatively warm, modified Circumpolar Deep Water to ice-shelf cavities. Here we identify potential oceanic gateways that could allow the access of warm water masses to Antarctic grounding lines based on critical access depths inferred from high-resolution bathymetry data. We analyse the properties of water masses that are currently present in front of the ice shelf and that might intrude into the respective ice-shelf cavities in the future. We use the ice-shelf cavity model PICO to estimate an upper limit of melt rate changes in case all warm water masses up to a certain depth level gain access to the cavities. We find that melt rates could increase in all regions at least by a factor of 2. Depending on the presence or absence of an oceanic gateway and the current ice-shelf melt conditions we find up to 200-fold larger melt rates. The identification of oceanic gateways is thus valuable for assessing the potential of ice-shelf cavities to switch from a 'cold' to a 'warm' state, which could result in widespread ice loss from Antarctica.

1 Introduction

The current mass loss from the Antarctic Ice Sheet is mainly triggered by thinning of the surrounding ice shelves (Pritchard et al., 2012; Paolo et al., 2015; Gudmundsson et al., 2019). Sub-shelf melting around Antarctica varies by orders of magnitude depending on the prevailing ocean conditions: a sub-shelf circulation that is initiated by sea-ice formation or tidal pumping (mode 1 or 3 in Jacobs et al., 1992, respectively) causes melt rates at the order of centimetres to a few metres per year. For example, area-averaged observed melt rates at Filchner–Ronne Ice Shelf are around $0.3 \pm 0.1\ \mathrm{m\,yr^{-1}}$ (Ronne) and $0.4 \pm 0.1\ \mathrm{m\,yr^{-1}}$ (Filchner) as estimated by Rignot et al. (2013). In these ice shelves, mode 1 melting plays a major role towards the grounding line and mode 3 melting near the ice-shelf front (Silvano et al., 2016). Where melting is driven by Dense Shelf Water (mode 1) or surface waters (mode 3), generally cold water masses are present within the cavity which can be hence classified as 'cold' – such as for Filchner–Ronne, Ross or Amery (Joughin et al., 2012; Silvano et al., 2016). Ice-shelf thinning and upstream mass loss are currently not observed in these cold-cavity regions (Joughin et al., 2012; Paolo et al., 2015; Greene et al., 2022). A

https://doi.org/10.5194/egusphere-2023-2583
Preprint. Discussion started: 27 November 2023

different mode of sub-shelf melting is driven by an inflow of water masses from the continental slope front (mode 2 in Jacobs et al., 1992), bringing water with temperatures well above the pressure-melting point into the ice-shelf cavity. Such cavities can be classified as 'warm' (Joughin et al., 2012). They typically experience melt rates at the order of tens of metres per year.

The exchange of water masses between the continental shelf and the open ocean is strongly influenced by bathymetry (Thoma et al., 2008; Nicholls et al., 2009; Hellmer et al., 2012; Pritchard et al., 2012; Tinto et al., 2019; Sun et al., 2022), but the processes that lead to on-shelf transport of warm water masses are highly complex and an active field of research. To what extent warm-water intrusions into ice-shelf cavities can be related to anthropogenic changes (Holland et al., 2022) or natural variability (Jenkins et al., 2016, 2018), remains to be determined. Once, however, warmer water masses enter an ice-shelf cavity, this can lead to a strong increase in sub-shelf melt rates and in further consequence cause the adjacent ice streams to thin, accelerate, and retreat. Highest thinning rates in Antarctica are found for ice shelves in the Amundsen Sea, where relatively warm, modified Circumpolar Deep Water (mCDW) can access the ice shelves at depth through submarine troughs (Nitsche et al., 2007; Walker et al., 2007; De Rydt et al., 2014; Mouginot et al., 2014; Jenkins et al., 2016; Millan et al., 2017; Naughten et al., 2023). This mCDW comprises relatively warm and salty water masses which reside at mid-depth, on average at around -500 m, in the Southern Ocean in front of the continental shelf (Schmidtko et al., 2014; Holland et al., 2020).

Ocean access to ice-shelf cavities is generally modulated by geological structures on the continental shelf that block or channel the distal intrusion of deeper and warmer water masses from north off the continental shelf, i.e. CDW. The abyssal ocean floor north of the Antarctic continent (here defined by $<$-1800 m) raises towards the continent to form the shallow continental shelf that has a mean depth of about -500 m (Heywood et al., 2014), with the transition zone being called the continental-shelf break (CSB). The width of the continental shelf, which is the distance from the CSB to the coastline or ice sheet, varies around Antarctica from tens of kilometres, in East Antarctica or the West Antarctic Peninsula, to hundreds of kilometres in the Ross or Weddell Sea (Heywood et al., 2014). While large data gaps still exist, recent Antarctic topography data incorporate major glacial troughs, ridges or other features of basal topography crosscutting the continental shelf (Arndt et al., 2013; Morlighem et al., 2020). These bathymetric features were mostly formed by erosion and sedimentation due to dynamic changes of the ice sheet during glacial cycles, e.g. ice streams leaving behind deep troughs when retreating (Bart, 2004; Hein et al., 2011; Morlighem et al., 2020).

The grounding line (or grounding zone, cf. Li et al., 2023), marks the transition between the grounded ice sheet and the floating ice shelves and thus constitutes the triple point of bedrock, ice, and ocean, see Fig. 1. Grounding lines in Antarctica can be found at depths down to -3000 m due to the effective erosion over long time scales. Sub-shelf melt rates are generally higher near the grounding line and lower towards the ice shelf's calving front. This general pattern is further modulated by exchanges with water masses within the cavity and through other dynamical processes at play (e.g. Coriolis). Ice-shelf thinning caused by melting close to the grounding line has been found to have the largest impact on the adjacent ice masses, resulting in higher fluxes across the grounding line due to a loss in buttressing (Reese et al., 2018b). For instance, Wouters et al. (2015) find a strong link between surface-lowering and an increase in the dynamical ice loss in the Southern Antarctic Peninsula since around 2009.

https://doi.org/10.5194/egusphere-2023-2583
Preprint. Discussion started: 27 November 2023

Distinct geological structures, such as troughs, are crucial boundary conditions for modelling ocean dynamics and the interaction of the ocean with the Antarctic Ice Sheet (Thoma et al., 2008; Hellmer et al., 2012), but only a few studies investigate the bathymetric access points or pathways to the grounding lines in detail and focus only on specific regions (see e.g. Herraiz-Borreguero et al., 2015; Tinto et al., 2019). Here, we present a simple approach to analyse *oceanic gateways* to the base of the Antarctic Ice Sheet, specifically to the ice-sheet's grounding lines. We identify oceanic gateways as the deepest topographic features that connect the deeper open ocean and the ice-shelf cavity, assuming that water follows this pathway, see Fig. 1. Where one or several deep troughs provide access to most of a region's grounding line, we identify this as a 'prominent' oceanic gateway. The temperature of water masses found along such pathways, along the ice-shelf front, and towards the open ocean provides information about the water masses currently present within ice-shelf cavities. They also inform about the water masses that could potentially access the cavity through these pathways, if the oceanic front at the continental-shelf break weakens and warm water masses intrude onto the continental shelf. We combine observations of bedrock topography and ocean water masses to assess the current as well as the potential melt in all Antarctic regions. While no dynamic changes are taken into account, our analysis serves as a first-order assessment of the maximum changes in ocean water temperatures and melt rates, expected by warm water intrusion at depth in Antarctica. Our approach of identifying relevant water masses that drive melting in cavities is also useful to improve the input for parameterisations of sub-shelf melt rates such as the ice-shelf cavity model PICO as suggested in Burgard et al. (2022).

In a related study, Kreuzer et al. (2023, in prep.) discuss potential changes in access depths and subsequent melt rates when considering relative sea-level changes resulting from deformational, gravitational, and rotational effects of the global redistribution of ice and ocean mass on glacial timescales.

We describe our methodology in Sect. 2, followed by a presentation of the results in Sect. 3. In Sect. 4 we discuss our approach and findings, with a general conclusion included in Sect. 5.

2 Methodology

First we introduce the oceanic gateways (Sect. 2.1), then describe the used ocean data (Sect. 2.2) and summarise how we diagnose sub-shelf melting with PICO (Sect. 2.3).

2.1 Identifying oceanic gateways from bathymetry

Our analysis is based on BedMachine v3 bathymetry (Morlighem et al., 2020; Morlighem, 2022). An oceanic gateway is a horizontal pathway from the open ocean to the grounding line of an ice-shelf cavity along the deepest possible ocean-connection between the two. The grounding lines, by our definition, encompass the grounded parts of the continental ice sheet. We identify oceanic gateways for 19 Antarctic regions based on the drainage basins defined in Zwally et al. (2012), with the Filchner–Ronne and Ross basins congregated as in Reese et al. (2018a). The oceanic gateways are derived from access depths calculated for every location on the Antarctic continental shelf and in the ice-shelf cavities. The *access depth* for each point on the continental shelf is the deepest level at which this point can be reached through successive flood-fill routines that start in the

https://doi.org/10.5194/egusphere-2023-2583
Preprint. Discussion started: 27 November 2023

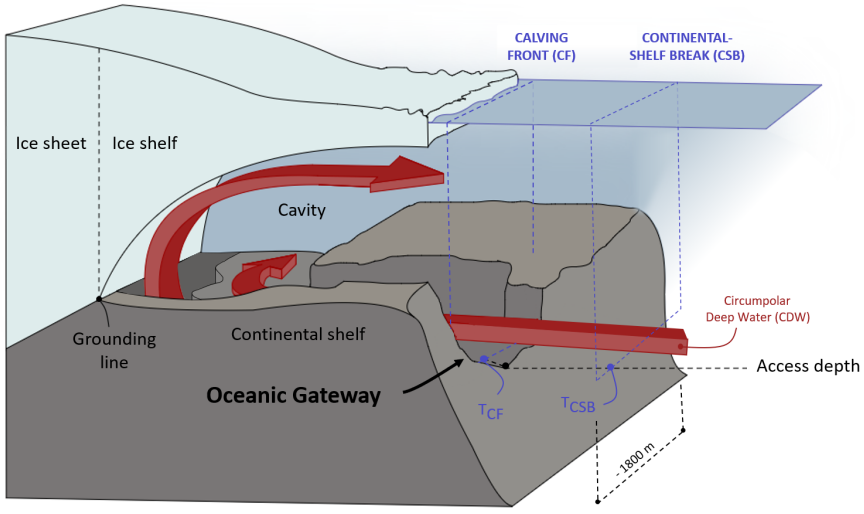

Figure 1. Schematic of an ice-shelf cavity system in Antarctica. Beyond the continental shelf, relatively warmer Circumpolar Deep Water is present. Its access to ice-shelf cavities is modulated by ocean circulation and bathymetry. Ocean temperatures at depth near the calving front (T_{CF}) yield information about the water masses that can already access the ice-shelf cavity. If a prominent oceanic gateway is present, water masses with a mean temperature T_{CSB} from the continental-shelf break (at the gateway's *access depth*) can potentially reach large parts of the grounding line of the respective ice shelf.

open ocean and iteratively 'fill' all neighbouring cells with bathymetry at the same or lower depth. The flood-fill is a common tool in the field of computer science and used for e.g. maze-solver simulators or computer graphics (Khudeev, 2005; Law, 2013; Kumar et al., 2020). As a result, our analysis yields circum-Antarctic access depths which are available as a 2D field on a 500 $\mathrm{m}\times$500 m grid horizontal grid spacing, following the resolution of the BedMachine data (Morlighem et al., 2020). A *critical access depth* $d_c(b,s)$ for each basin b is identified such that a substantial part g of its grounding lines are accessible (with 10 % $\leq g \leq$ 90 %, varied in steps of 5 % in our analysis, see Fig. 3). We only consider the grounding lines which are connected to the continental ice sheet, excluding larger islands and ice rises. With our analysis, we are then able to compare at which critical depth the typically deep-lying grounding lines of fast-flowing ice streams are reached.

2.2 Ocean properties

We analyse the properties of water masses based on the ISMIP6 ocean temperature and salinity climatology (Jourdain et al., 2020). The dataset is available at a 8 km x 8 km horizontal and 60 m vertical resolution. The data points indicate temperatures and salinities averaged over the period 1995–2017. While observational datasets have many data gaps and thus do not provide sufficient horizontal as well as vertical coverage (especially on the continental shelf), the ISMIP6 dataset is generated similar

https://doi.org/10.5194/egusphere-2023-2583
Preprint. Discussion started: 27 November 2023

to our flood-fill approach: While accounting for topographic barriers, the temperature and salinity fields from observations are flooded into the ice-shelf cavities and regions below sea level that are currently covered by grounded ice. Due to this approach and the extended spatial coverage, we consider the ISMIP6 ocean dataset to be very well suited for our study. We extract ocean properties near the ice shelf's calving front, along the oceanic gateways as well as along the continental-shelf break, based on the critical access depths $d_c(b,g)$ for each basin $b = 1, 2, ...19$, that we test for different percentages of grounding line access $g = 10, 15, ...90\%$ that define the access depths. The temperatures in front of the ice shelves (at the calving front) serve as a proxy for ocean water masses that can currently reach the ice shelves' deep grounding lines (similar to mode 1 melting in Silvano et al., 2016). The calving front (CF) is defined through the native BedMachine mask as the boundary between floating (or grounded) ice and the ocean. We calculate horizontal averages along this transect at the critical access depth of the basin and define T_{CF} and S_{CF} as

$$T_{\mathrm{CF}}(b,g) = \mathrm{mean}\left\{ T(x,y,z) \middle| (x,y) \in \mathrm{CF} \text{ and } z = d_c(b,g) \right\} \tag{1}$$

and

$$S_{\mathrm{CF}}(b,g) = \mathrm{mean}\left\{ S(x,y,z) \middle| (x,y) \in \mathrm{CF} \text{ and } z = d_c(b,g) \right\}. \tag{2}$$

In a second step, we derive properties along the continental-shelf break (CSB) at the critical access depth for each basin. We define the CSB to lie at the horizontal coordinates where the bathymetry is -1800 m deep (i.e. along the -1800 m isobath). These are ocean water masses that could potentially enter the ice-shelf cavity once an oceanic gateway towards the grounding line exists. We define the average temperature and sanility along this transect as T_{CSB} and S_{CSB}, respectively as

$$T_{\mathrm{CSB}}(b,g) = \mathrm{mean}\left\{ T(x,y,z) \middle| (x,y) \in \mathrm{CSB} \text{ and } z = d_c(b,g) \right\} \tag{3}$$

and

$$S_{\mathrm{CSB}}(b,g) = \mathrm{mean}\left\{ S(x,y,z) \middle| (x,y) \in \mathrm{CSB} \text{ and } z = d_c(b,g) \right\}. \tag{4}$$

2.3 Sub-shelf melting diagnosed via ice-shelf cavity model PICO

We use T_{CSB} and T_{CF} as well as corresponding salinities S_{CSB} and S_{CF} for diagnosing sub-shelf melt rates with the Potsdam Ice shelf cavity mOdel (PICO, Reese et al., 2018a). PICO extends the ocean box model by Olbers and Hellmer (2010) to be applicable in 3D-ice sheet models. It mimics the vertical overturning circulation present in ice-shelf cavities and can reproduce the wide range of average observed melt rates for 'warm' and 'cold' cavities. Ocean input is considered in PICO as an average per basin and once water masses reach the grounding line, they rise along the ice-shelf base towards the calving front, driven by the ice pump (Lewis and Perkin, 1986). PICO model parameters $C = 3.0\,\mathrm{Sv\,m^3\,kg^{-1}}$ that describes the strength of the vertical overturning circulation, heat exchange coefficient $\gamma_T^* = 7 \times 10^{-5}\,\mathrm{m\,s^{-1}}$, as well as the maximum number of boxes (N = 5) are used as in Reese et al. (2023). These parameters are tuned to represent the sensitivity of melt rates to ocean temperature changes (cf. Reese et al., 2023). Input is based on temperature and salinity observations compiled by Schmidtko et al. (2014). In the

https://doi.org/10.5194/egusphere-2023-2583
Preprint. Discussion started: 27 November 2023

tuning process, temperatures on the continental shelf were corrected for, similarly to the approach by Jourdain et al. (2020), such that the melt rates calculated by PICO match present-day observations compiled by Adusumilli et al. (2020).

The ice-shelf cavity model is implemented in the Parallel Ice Sheet Model (PISM; https://www.pism.io; Bueler and Brown, 2009; Winkelmann et al., 2011). As initial conditions, we use ice thickness and bed topography from the BedMachine v3 dataset on a 4 $\mathrm{km}\times4$ km grid spacing. We compare our obtained melt rates to recent estimates by Adusumilli et al. (2020) that derive circum-Antarctic melt rates from satellite-borne laser altimetry.

3 Results

Figure 2 shows the map of access depths for all locations on the Antarctic continental shelf and its ice-shelf cavities. While some ice-shelf cavities have spatially varying access depths (such as Ross Ice Shelf), others have one access depth throughout their cavity and up to the grounding lines. Generally, the regions that show the latter behaviour can be accessed by single oceanic gateways. For instance, the Filchner–Ronne and Amery regions both feature one prominent gateway at -595 m and -525 m respectively, where 75 % or 60 % of the grounding lines are reached correspondingly at one distinct, deep, critical depth level. To calculate the critical access depth for the individual basins, we assume that the gateway(s) provide access to a significant amount of the grounded Antarctic Ice Sheet e.g. for $d_c(g = 50\ \%, b)$ in Fig. 2. When large portions of the grounding lines are reached by the flood-fill algorithm at the same depth level, i.e. reached by water at the same depths, a prominent oceanic gateway can be detected. The deepest critical access levels can be found for the Filchner–Ronne (basin 1) and Amery (basin 6) regions, as well as in the Amundsen Sea region, and in parts of the Ross Ice Shelf. The critical access depth for a 50 % grounding line access range from -595 m for Filchner–Ronne Ice Shelf to -75 m at the Western Antarctic Peninsula. Figure 3 shows the resulting critical access depths for each basin with increasing portions of the grounding line being reached, starting at the deepest levels. In most basins, the identified gateways provide the deepest access depths found in the respective cavities. The Ross Ice Shelf (basin 12) shows two prominent gateways with a critical access depth at -570 m and -500 m. At Fimbul Ice Shelf (basin 3) we find less prominent gateways at -425 m and -390 m, at the Baudoin/Lazarev region (basin 4) at -420 m,-380 m, -360 m and -215 m, near Totten Glacier (basin 8) at -495 m and -370 m, and at Cook/Mertz Ice Shelf (basin 9) we detect an oceanic gateway at -465 m. In the Amundsen Sea (basin 14) we find a deep oceanic gateway at -575 m and at Abbot/Cosgrove Ice Shelf at -335 m (basin 15).

3.1 Ocean properties extracted at critical access depths

Temperatures along the ice-shelf fronts, $\mathrm{T_{CF}}$, which are evaluated at the critical access depth of the individual basins are generally lower than temperatures found at the same depth at the continental-shelf break, $\mathrm{T_{CSB}}$ (for $g = 50$ %, see Fig. 2). $\mathrm{T_{CSB}}$ is much warmer than $\mathrm{T_{CF}}$ because it incorporates the warm CDW which resides at that depth off the Antarctic continent. Temperatures $\mathrm{T_{CF}}$ and $\mathrm{T_{CSB}}$ at the Pacific side of the Antarctic coast are about 1 to 2 °C warmer than the other regions in our dataset, especially in the Bellingshausen Sea (cf. Fig. 2). When we assume that 50% of the grounding line is accessed by warm ocean waters ($g = 50$ %), the difference between the temperatures near the calving front, $\mathrm{T_{CF}}$, and the continental-shelf

https://doi.org/10.5194/egusphere-2023-2583
Preprint. Discussion started: 27 November 2023

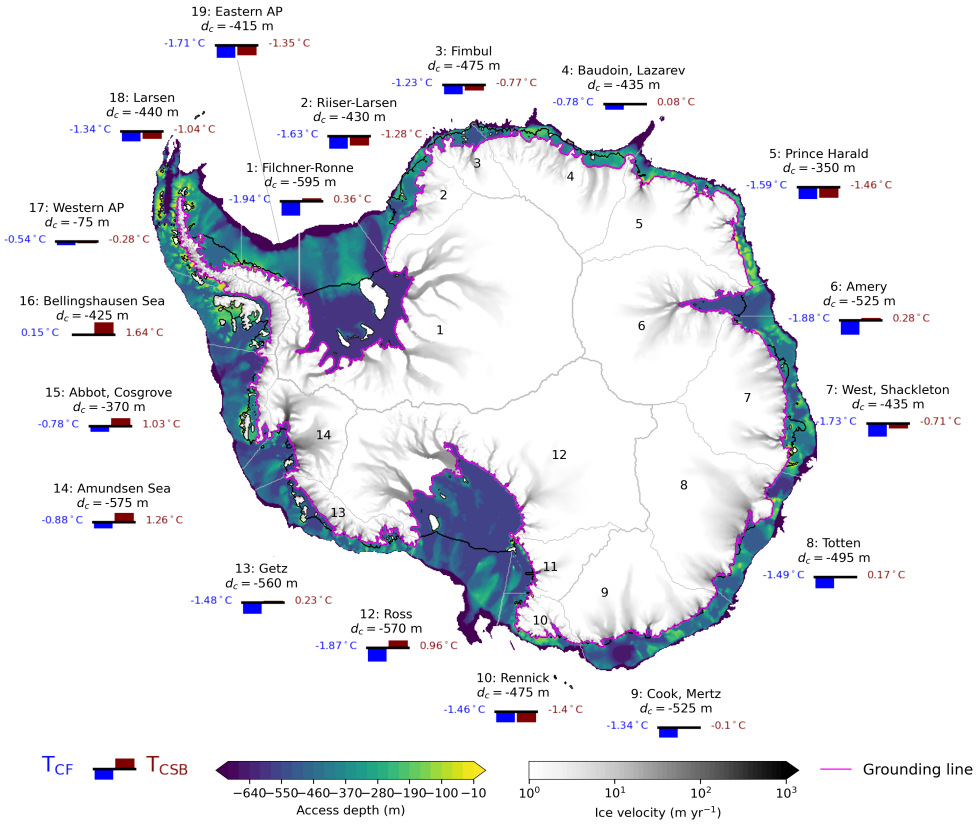

Figure 2. Access depths around Antarctica. Color shading indicates the access depth over the continental shelf and in the ice-shelf cavities, based on BedMachine v3 Antarctica topography data (Morlighem et al., 2020). The critical access depth d_c is shown for reaching $g = 50$ % of the respective cavities' grounding lines. The drainage basins (grey outlines) are based on Zwally et al. (2012), consolidated as in Reese et al. (2018a), and labelled according to prominent ice shelves (with AP = Antarctic Peninsula). The respective temperatures near the present-day ice-shelf calving fronts, T_{CF}, and at the continental-shelf break, T_{CSB}, are marked in blue and red, respectively. Speed of grounded ice in grey shading showing major ice streams, taken from Mouginot et al. (2019). Magenta line delineates the ice sheet's grounding line.

break, T_{CSB}, can mount to 2.8°C as for instance for the Ross Ice Shelf region. The difference between the two temperature estimates is much smaller (≤ 1.0°C) in Dronning Maud Land (basins 2 to 5) which is a consequence of the narrow continental shelf and hence the small distance between the calving front and continental-shelf break, as identified in our study. Figure 4 shows the ocean conditions T_{CF}, T_{CSB}, S_{CF} and S_{CSB} obtained when requiring different percentages, g, of grounding line access in the flood-fill algorithm. The difference in temperatures T_{CSB} - T_{CF} is especially large for the basins that we find to feature a prominent gateway or several gateways, such as Filchner–Ronne (basin 1), Amery (basin 6), and Ross (basin 12). In those regions, the difference in the temperatures is >2°C. Also for the regions with smaller detected gateways (e.g. basins

https://doi.org/10.5194/egusphere-2023-2583
Preprint. Discussion started: 27 November 2023

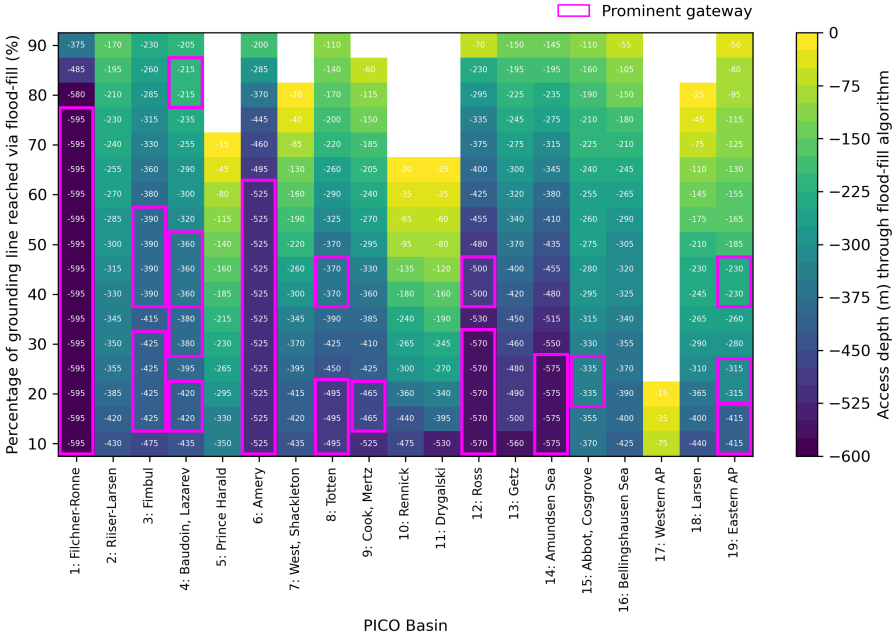

Figure 3. Critical access depths for varying fractions of the grounding lines to be reached. Thick magenta lines highlight the access to the ice-shelf region over a prominent oceanic gateway. White spaces indicate that not all grounding lines of this region can be reached via a flood-fill from the open ocean, meaning that some parts of the grounding lines are situated above 0 m. AP = Antarctic Peninsula.

4, 9, 15 or 19), the difference is very pronounced, particularly at a low percentage of grounding line access. If those parts of the grounding line also have the highest grounding line depths, warm water intrusion at depth could cause significant melting in the region. In most basins, the waters masses from the continental-shelf break are saltier than compared to those near the calving front (S_{CSB}>S_{CF}). The difference in the extracted salinity inputs is however small, ranging between -0.18 PSU (for high g in basin 18) to 0.51 PSU (for low g in basin 13), see Fig. 4.

For the Western Antarctic Peninsula (basin 17) we refrain from deriving critical temperature and salinity estimates for both the calving front and the continental-shelf break due to the region's shallow access depth, see Fig. 3. As the Drygalski region (basin 11) shares the continental-shelf break with the Ross region, we also do not provide an estimate for T_{CSB} here. For both regions, subsequent melt rates are not estimated due to lacking temperature and salinity input.

3.2 Change in melt rates assuming warm water intrusion at critical access depth

The diagnosed sub-shelf melt rates with PICO for the ocean temperatures and salinities along the calving front, as well as the continental-shelf break as obtained in the previous section, are displayed in Fig. 5. All regions show a strong increase in sub-shelf melting when assuming that warm waters from the continental-shelf break can reach the ice-shelf cavities. Mean basal melt rates for $g = 50$ % grounding line access are highest for the Bellingshausen and Amundsen Sea basins reaching 40.4

https://doi.org/10.5194/egusphere-2023-2583
Preprint. Discussion started: 27 November 2023

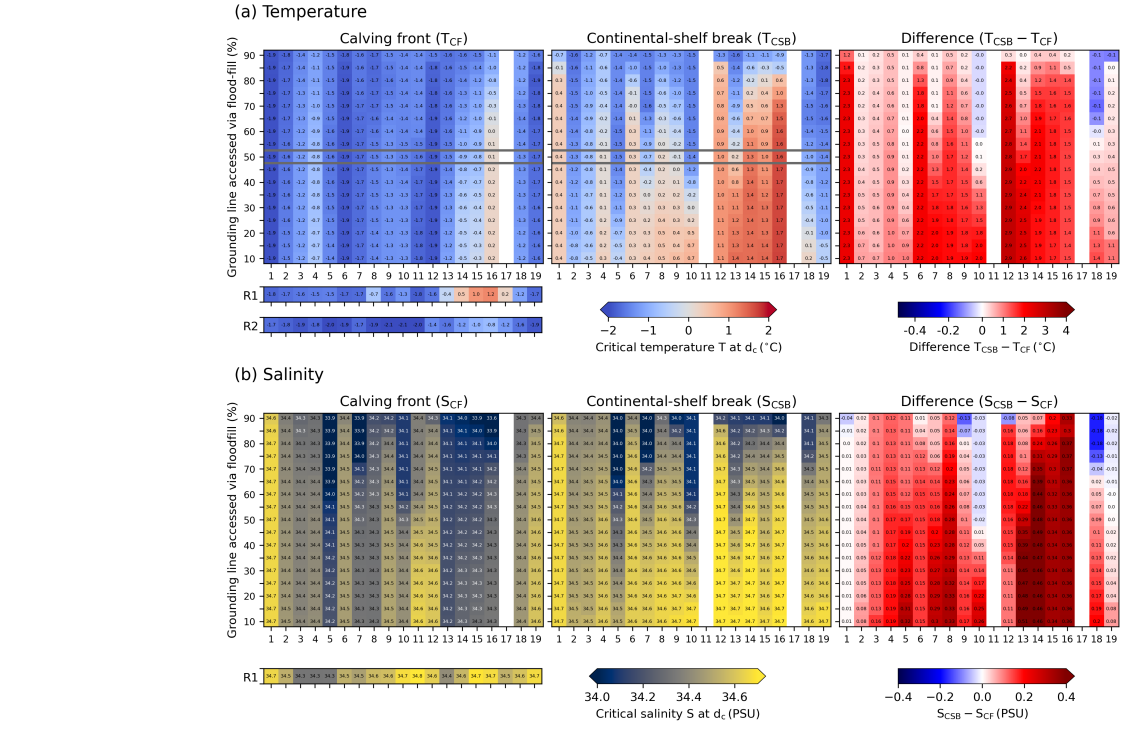

Figure 4. Assessment of extracted ocean conditions (temperature and salinity). **(a)** Derived temperatures T_{CF} (at the calving front), T_{CSB} (at the continental-shelf break) and the difference between these two estimates for all 19 PICO regions. Temperatures are evaluated at the access depths which correspond to a specific grounding line access (% of total grounding line reached), which result from the flood-fill algorithm, see Fig. 3. Grey boxes highlight the temperatures that are displayed in Fig. 2 and correspond to $g = 50$ % grounding line access. **(b)** Corresponding salinity estimates and differences. R1 and R2 refer to basin averaged temperatures from Reese et al. (2018a) and Reese et al. (2023), respectively, that were formerly used as PICO input temperatures (or salinity).

and 68.3 $\mathrm{m\,yr^{-1}}$, respectively. The relative change in basal melt rates between the two origins considered here (CF and CSB) is strongest in regions that featured 'cold' cavities at present (cf. Fig. 4, basin 1,6 or 12). The increase in melting is mainly driven by the changes in temperature: the melting effect of the salinity differences of around 0.2 PSU as extracted here, are by around one order of magnitude smaller.

In the following we are looking more closely at the oceanic gateways to major Antarctic ice shelves, while comparing the results from our analysis to existing observations and regional modelling studies.

https://doi.org/10.5194/egusphere-2023-2583
Preprint. Discussion started: 27 November 2023

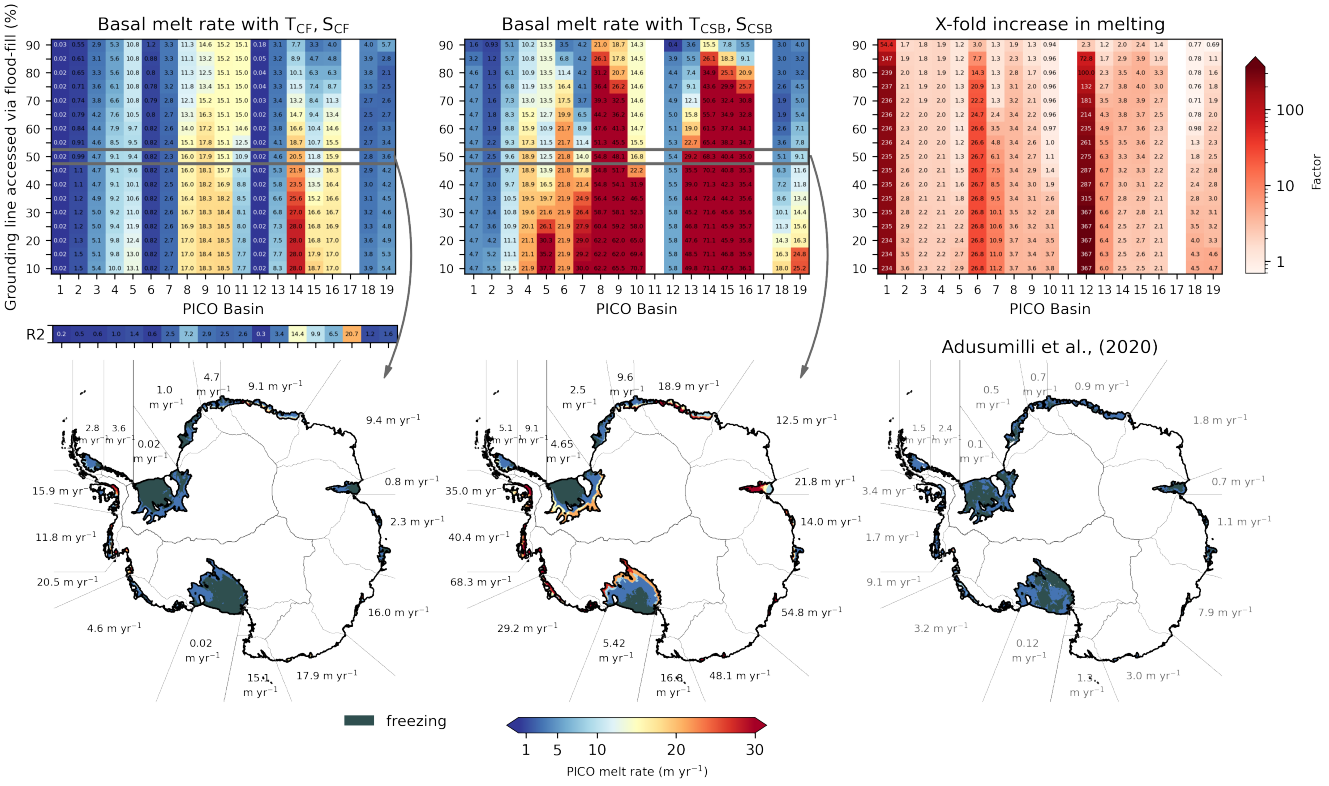

Figure 5. Circum-Antarctic PICO sub-shelf melt rates. Melt estimates are shown for the temperature and salinity input derived from the calving front (left), from when assuming warm water intrusion from the continental-shelf break (middle) and an estimate of the difference between these two (right) for all 19 Antarctic regions. Maps show the spatial fields of basal melt rates. The corresponding critical access depth, at which the ocean input is evaluated, is here given for $g = 50$ % in the corresponding basin. These estimates correspond to the critical temperatures depicted in Fig. 2 and salinity values included in Fig. 4. Dark grey shading indicates regions with refreezing, which occurs in larger ice-shelf regions like Filchner–Ronne and Ross. Labels refer to basin mean melt rate.

3.3 Oceanic gateways to major Antarctic ice shelves

3.3.1 Filchner–Ronne Ice Shelf

At the Filchner–Ronne Ice Shelf, we identify a prominent oceanic gateway along Filchner Trough (see Fig. 6 c), through which 75 % of the grounding line is reached at -595 m (compare Fig. 3). The mean depth of the basin's grounding lines lie at around
195 -1000 m, so that at a critical depth of -595 m reaches much of the grounding line already. The deepest grounding lines are found down to around -2000 m in the BedMachine dataset (see Fig. 6 b). The Filchner Trough is a characteristic feature of the submarine topography in the Filchner–Ronne Ice Shelf region, extending from around Foundation Ice Stream to more than 450 km into the Southern Weddell Sea (distance measured from the ice-shelf front and taken from Larter et al., 2012). Its width

https://doi.org/10.5194/egusphere-2023-2583
Preprint. Discussion started: 27 November 2023

varies between 125 to 175 km (Larter et al., 2012) and it terminates with a sill on its end towards the Weddell Sea (Hellmer et al., 2012). The sill depth determines the region's access depth in our study.

At present, Filchner–Ronne Ice Shelf has a relatively cold cavity, with observed melt rates around $0.32 \pm 0.1\ \mathrm{m\,yr^{-1}}$ (Rignot et al., 2013). It currently contributes 10 % of the total basal mass flux around Antarctica (Mueller et al., 2018). In our analysis, water masses along the Filchner–Ronne calving front are close to the pressure melting point (with T_{CF}= -1.94°C at the critical access depth, cf. Fig. 6 d). A slope front in front of the ridge in Filchner Trough (Fig. 6 c) currently blocks warmer water masses that are present along the continental shelf (T_{CSB}= 0.36°C at the critical access depth, Fig. 6 e) from entering the cavity. If these could enter the cavity, Filchner–Ronne would transition from a 'cold' to a 'warm' cavity, as also modelling studies suggest (Joughin et al., 2012; Hellmer et al., 2012, 2017). At present, high-salinity shelf water (HSSW) is flowing into the ice-shelf cavity from the Ronne basin, while ice-shelf water (ISW) mainly flows outward through Filchner Trough (Nicholls et al., 2009; Naughten et al., 2021; Darelius et al., 2023). In our analysis, we also find colder HSSW residing in front of the sill of Filchner Trough on top of warmer water masses at depth, see (Fig. 6 c). Hellmer et al. (2012) found that a redirection of the slope current through Filchner Trough could occur within the 21st century under high greenhouse gas emissions. Naughten et al. (2021) find a two-timescale response of the Filchner–Ronne Ice shelf under climate change, where warm water begins to intrude into the cavity only at approximately 7°C warming above pre-industrial levels. As for the drivers for such a regime shift, Haid et al. (2022) find that the density balance between the shelf waters originating from sea-ice production and the warmer water at the continental-shelf break as the most decisive factor for the Filchner–Ronne ice-shelf cavity to tip into a warm state.

For the temperature and salinity input with the origin of the calving front of the Filchner–Ronne basin, melt rates of about $0.02\ \mathrm{m\,yr^{-1}}$ (for $g < 90$ %) can be inferred. When assuming that warm water masses from the continental-shelf break reach all the way into the cavities, melt rates are two orders of magnitude higher and reach up to $4.65\ \mathrm{m\,yr^{-1}}$ on average, which roughly correspond to the warm melt mode found at present near Getz Ice Shelf (cf. Reese et al., 2018a; Adusumilli et al., 2020).

3.3.2 Amery Ice Shelf

Towards Amery Ice Shelf, we identify a gateway through Prydz Channel at a critical depth of -525 m. According to our algorithm up to 60 % of the region's grounding line is reached at this depth. Mackintosh et al. (2014) analyse the retreat history of the East Antarctic Ice Sheet since the Last Glacial Maximum, highlighting that the Amery grounding zone has retreated along Prydz Channel. This is an example that shows that gateway-like features such as Prydz Channel can often times be linked to glacial erosion.

The grounding line of Amery Ice Shelf lies very deep, at a mean depth of around -1100 m in the BedMachine dataset, while the deepest parts of the grounding line are found at -2950 m depth (see Fig. 7 b). Rignot et al. (2013) list observed melt rates at Amery Ice Shelf as $0.6 \pm 0.4\ \mathrm{m\,yr^{-1}}$. The temperatures for a $g = 50$ % level grounding line access (the prominent gateway provides access at already $g > 50$ %) near the calving front are -1.88°C, and 0.29°C at the continental-shelf break (evaluated at -525 m). The subsequent melt rates are $0.8\ \mathrm{m\,yr^{-1}}$ and $21.8\ \mathrm{m\,yr^{-1}}$, respectively. The obtained melt rates for present-day conditions, when considering water masses from near the calving front, are therefore within the given observational uncertainty. If warm Circumpolar Deep Water residing at the continental-shelf break will actually pass through the identified

https://doi.org/10.5194/egusphere-2023-2583
Preprint. Discussion started: 27 November 2023

gateways remains uncertain. Williams et al. (2016) find a different pathway of modified Circumpolar Deep Water towards Amery Ice Shelf, through Four Ladies Bank more to the East, see Fig. 7 a. Amery Ice Shelf is located downstream of Lambert glacier that is draining about 16 % of the grounded East Antarctic Ice Sheet (Fricker et al., 2000). Enhanced melting due to warm water intrusion at depth could hence produce an increase in sea-level rise contribution from large portions of the East Antarctic Ice Sheet.

3.3.3 Ross Ice Shelf

We identify two oceanic gateways towards Ross Ice Shelf, see Fig. 3, as well as spatially varying access depths throughout the cavity (Fig. 8 a). With regards to the grounding line access, deep access depths are found near Siple Coast. Grounding lines near the Transantarctic Mountains (TAM), near Byrd Glacier, are located in shallower regions (Fig. 8 b), that thus feature shallower access depths. For the majority of the cavity, we identify the Glomar Challenger Basin (Fig. 8) as the topographic feature which provides access to the cavity at the depth of -570 m. The basin is a north-east trending cross-shelf paleo-trough (Owolana, 2011). We determine its lower lying western sub-basin as an important gateway, that provides access to around 30 % of the basin's grounding line. At -570 m, the grounding lines of Mac Ayeal, Bindschadler and Mercer/Willans Ice Streams (Western side) are reached as well as the grounding line of Byrd Glacier on the eastern side of Ross Ice Shelf. The mean depth of the basin's grounding lines is rather shallow at around -575 m, but can reach around -1000 m in the BedMachine dataset (see Fig. 8 b). These deep-lying grounding lines are accessed at the critical depth of -570 m, see Fig. 8 b. As mentioned above, highest melt rates can be expected in those deep grounding line regions due to the lower pressure melting point and therefore higher thermal forcing. Similar to FRIS, cold water masses are found along the ice-shelf front (Fig. 8 d) with warmer water masses beyond the continental slope front (Fig. 8 e). The derived temperatures are at -1.48°C near the calving front and 0.96°C at the continental-shelf break, when $g = 50$ %. These temperatures correspond to PICO melt rates of 0.02 $\mathrm{m\,yr^{-1}}$ for the calving front conditions and up to 5.42 $\mathrm{m\,yr^{-1}}$ in a scenario of warm-water intrusion. Observed melt rates lie at 0.0 ± 0.1 $\mathrm{m\,yr^{-1}}$ for the Western and 0.3 ± 0.1 $\mathrm{m\,yr^{-1}}$ for the eastern part of the ice shelf (Rignot et al., 2013). The Ross basin can hence be classified as a 'cold' cavity, like Filchner Ronne Ice Shelf. Melt rates, inferred by our analysis, have the same order of magnitude as present-day observed rates. Kenneally and Hughes (2004) state that largest observed melt rates are about 12 ± 2 $\mathrm{m\,yr^{-1}}$ near Byrd Glacier's grounding line. Tinto et al. (2019) find that high-salinity shelf water flows under the ice front near Ross Island to the East, then moves southward towards the East Antarctic side of the ice shelf, and eventually exits through Glomar Challenger Trough to the Ross Sea. They highlight that the tectonic boundary between the East and West Antarctic side of Ross Ice Shelf impact the vulnerability to sub-shelf melting, since the part of the cavity near Siple Coast is rather isolated from the influence of in-flowing (warm) water masses. Here we assume, however, an inflow of warm water masses through Glomar Challenger Basin reaching those ice streams, given an access of water masses at the critical depth of -570 m. Nonetheless, the rest of the cavity near Siple Coast shows generally more shallow access depths in our analysis, which can be linked to the tectonic boundary and the difference in the crustal composition that influence the bathymetry (Tinto et al., 2019).

https://doi.org/10.5194/egusphere-2023-2583
Preprint. Discussion started: 27 November 2023

3.3.4 Ice shelves in the Amundsen Sea

In the Amundsen Sea region, we find an oceanic gateway to Pine-Island and Thwaites glaciers along the Abbot and Cosgrove Trough with a critical access depth of -375 m (Fig. 9). Abbot Cosgrove Trough is a -760 m deep feature that evolved through erosion along a paleo ice stream across the continental shelf (Hochmuth and Gohl, 2013; Klages et al., 2015). The mean depth of this basin's grounding line is at around -680 m, but the deepest parts lie at <-1500 m, that are reached by the access depth via the gateway. Warm water masses are present along the entire transect along the proposed gateway up to the ice-shelf front (Fig. 9 c), in front of the continental shelf (Fig. 9 e), and in the bathymetric depressions along the ice-shelf fronts (Fig. 9 d). We obtain temperatures of -0.88°C near the calving front and of 1.26°C at the continental-shelf break for a 50 % grounding line access. Pine Island glacier with observed melt rates of 16.2±1.0 $\mathrm{m\,yr^{-1}}$ and Thwaites glacier with 17.73±1.90 $\mathrm{m\,yr^{-1}}$, respectively, have been considered belonging to one basin in our analysis. When using the ocean conditions along the calving front for the analysis, we find melt rates of 20.5 $\mathrm{m\,yr^{-1}}$ (for $g = 50$ %). The melting could increase to 68.3 $\mathrm{m\,yr^{-1}}$ when assuming that warm water from the continental-shelf break accesses 50 % of the basins grounding line. At present, ice shelves in the Amundsen Sea have warm cavities and therefore dominate the current mass loss in Antarctica (see e.g. Pritchard et al., 2012), indicating that this region is out of balance with the current oceanic forcing. Thoma et al. (2008) simulate CDW intrusion onto the Amundsen shelf and find that the warm water reaching Pine Island Bay are guided trough a submarine trough reaching to the continental-shelf break, close to where the continental-shelf break temperatures T_{CSB} are estimated in our study (see green dots in Fig. 9 a). Haigh et al. (2023) find that the ridge that is indicated in our study as the overflow point (see Fig. 9 c), blocks inflow from the Bellingshausen Sea at depth, so that water masses rather originate from the Pine Island Thwaites Trough, similar to Thoma et al. (2008). Gómez-Valdivia et al. (2023) employ a global climate model and find a shift in currents in the Amundsen Sea sector, leading to an enhanced onshore transport of CDW and an increase in ocean temperatures by 1.2°C. This estimate is of the same order of magnitude as the difference in critical temperatures, T_{CSB} - T_{CF}, that we obtain with our algorithm (cf. Fig. 4).

3.3.5 Ice shelves in the Totten region

In East Antarctica, for instance, we identify a gateway towards Totten Ice Shelf through a trough near the Law Dome peninsula, that provides access to 20 % of the grounding line at -495 m (see Fig. A1 in the Appendix). The mean depth of the basin's grounding line is around -635 m, but the deepest parts go down to <-2500 m. Those deep parts of the grounding line are accessed at -495 m according to our analysis. In the ISMIP6 climatology, warm temperatures are not only present along the continental-shelf break but can also be found on the continental shelf in front of Totten Glacier (cf. Fig. A1, c and e). This fits to the findings in Nitsche et al. (2007) who compare CTD measurements with temperatures from the same dataset. Vaňková et al. (2023) find spatially varying melt rates ranging from 0.4 $\mathrm{m\,yr^{-1}}$ to over 20 $\mathrm{m\,yr^{-1}}$ underneath Totten Ice Shelf and an inter-annual variability of 7 to 9 $\mathrm{m\,yr^{-1}}$, using radar measurements. Others find melt rates at Totten Ice Shelf to be 10.47±0.7 $\mathrm{m\,yr^{-1}}$ (Rignot et al., 2013). From our algorithm we obtain melt rates at 16.0 $\mathrm{m\,yr^{-1}}$ when considering temperatures and salinities from the calving front (CF) and a $g = 50$ % grounding line access. According to our analysis, melt rates at Totten would see

https://doi.org/10.5194/egusphere-2023-2583
Preprint. Discussion started: 27 November 2023

an around 3.5-fold increase in melt rates (to 54.8 $\mathrm{m\,yr^{-1}}$), when assuming warm water intrusion at the critical depth where 50 % of the grounding lines are reached (at -495 m). Totten Ice Shelf is the floating extension of Totten Glacier, that drains a catchment containing ice with an equivalent of 3.5 m of global sea-level potential (Greenbaum et al., 2015), and currently experiences the largest thinning rate of all East Antarctic regions (Pritchard et al., 2009; Flament and Rémy, 2012; Greenbaum et al., 2015). Here, elevated sub-shelf melt rates due to warm water intrusion onto the continental shelf could already be the cause for the adjacent glacier to thin. Further ocean-induced melting can therefore have significant consequences to global sea-level rise. Adding to that, Herraiz-Borreguero and Naveira Garabato (2022) analyse ocean observations showing that mid-depth CDW has warmed off coast of the East Antarctic Ice Sheet. This warming can be associated with a poleward shift of the westerlies potentially leading to an intensified oceanic heat supply to East Antarctica.

4 Discussion

Our data analysis infers potential pathways for warm water intrusion into ice-shelf cavities and their corresponding 'critical access depths' for 19 drainage basins in Antarctica.

The results of the analysis need to be evaluated in the light of the key assumptions and limitations of our approach: firstly, we assume that ocean waters in front of the ice shelf serve as valid proxy for water masses that currently drive melting underneath the ice shelf, which is generally valid for cold-mode ice shelves (Silvano et al., 2016). Second, we estimate the continental-shelf break temperatures at the same depth, assuming that flow simply follows the bathymetry, and not, e.g., isopycnals (Drijfhout et al., 2013). Ocean dynamics, which crucially determine sub-shelf circulation patterns and thereby influence the access potential (Nicholls et al., 2009; Williams et al., 2016), are not considered in this study. Our analysis is thus a sole representation of the role of the geometry of the continental shelf including the ice-shelf cavities and connecting features such as the oceanic gateways. Our study could therefore be improved by considering specific ocean circulation patterns informed by high-resolution ocean models.

Cold and dense shelf waters flowing out of ice-shelf cavities generally shield the ice shelf from warm CDW intrusion at depth (Janout et al., 2021). The circulation patterns in the ice-shelf cavity system such as Filchner–Ronne, are strongly controlled by dynamical processes, such as e.g. Coriolis or, for instance, the interplay of sea-ice production and polynya formation which is in turn linked to anomalies in the large-scale atmospheric circulation around Antarctica (Alley et al., 2015; Janout et al., 2021; Haid et al., 2022). However, our identified gateways could be an entry point to cross-cut the density barrier in front of the continental shelf (Hirano et al., 2023). Furthermore, changes in the thermocline depth could also lift up water masses over topographic features (Assmann et al., 2013; Dutrieux et al., 2014; Hattermann, 2018; Daae et al., 2020).

Typically, if CDW flows onto the continental shelf, it mixes with fresh and colder on-shelf water masses (Wang et al., 2023). This modified Circumpolar Deep Water (mCDW) is generally colder than the critical temperatures estimated in this study. Here, however, we neglect the modification of Circumpolar Deep Water when accessing the grounding lines in the ice-shelf cavities.

https://doi.org/10.5194/egusphere-2023-2583
Preprint. Discussion started: 27 November 2023

In addition to these overarching structural uncertainties, additional uncertainties arise from the methodology and data: our flood-fill algorithm is based on the bathymetric structures and characteristics which are represented in the BedMachine data. We apply our algorithm on the dataset grid resolution (at a 500 $\mathrm{m}\times500$ m grid spacing) which we think is crucial to preserve features that are resolved at that scale. Even higher resolutions would allow a more precise analysis of the topographic structures, but this would require higher computational resources, and main features of present oceanic gateways are well-resolved at the current grid spacing. As the oceanic gateways may require a certain width for the dynamic inflow of ocean water, even higher resolutions may not provide more reasonable insights. We further assume that the bathymetry is time-invariant, which is not the case when considering longer time scales. Sill depths and grounding line location and thus access depths may change by hundreds of meters in response to erosion, sea-level changes and glacial isostatic adjustment effects (cf. Kreuzer et al., 2023, in prep.).

Cavity-resolving ocean models are computational very expensive and therefore limited to simulations on centennial timescales. Large-scale modelling studies thus often rely on parameterisations to infer ocean-driven sub-shelf melting. We here use the PICO model to estimate sub-shelf melt rates based on the temperatures and salinities in front of the ice shelves as well as from the continental shelf-break. Favier et al. (2019) find that a box parameterisation that mimics the vertical overturning in the cavity, such as PICO, gives good results when comparing to coupled ice-ocean simulations. However, our melt rate estimates could be altered when using a different melt parameterisation or assuming a higher melt rate sensitivity to thermal forcing, e.g. by using a quadratic melt relationship (Burgard et al., 2022).

Furthermore, we use one fixed parameter combination for the overturning and heat exchange coefficients in PISM-PICO, to show the order of magnitude of warm water intrusions from the continental-shelf break. We use those particular parameters that were selected to match the sensitivity of melt rates to temperature changes for present-day Antarctica (Reese et al., 2023). However, a full model ensemble would be required to estimate the uncertainty that arises from the choice of the PICO parameters.

Moreover, with our approach, adjusting PICO input temperatures so that melt rates match present-day observations (cf. Reese et al., 2023) may not be required any longer. A comparison of formerly employed input temperatures and the critical temperatures extracted in this study can be found in the Appendix, Fig. A2. Especially in the Pacific facing regions, such as the Amundsen Sea sector, the calving front conditions extracted here match well the adjusted temperatures from Reese et al. (2023), that are lower than in Reese et al. (2018a). In addition, we consider using a 4 $\mathrm{km}\times4$ km grid spacing for estimating basal melt rates a good compromise between having a high resolution at the grounding line, on the one hand, and computational feasibility on the other hand.

When using the existing definitions of the PICO basins to subdivide the Antarctic regions for our analysis, we use the approach of Reese et al. (2018a) where the drainage basins by Zwally et al. (2012) were mainly extended along meridians into the ocean. In the Filchner–Ronne region, these basin boundaries for example do not cover the overflow point at the sill at Filchner Trough (cf. Fig. 6 a). In another case, in the Amundsen Sea, the small portion of the continental-shelf break extracted from the basins boundary may not adequately represent the ocean conditions influencing the glaciers in the regions. Our analysis of the oceanic gateways could help to better inform the basin boundaries for different melt parameterisation in

https://doi.org/10.5194/egusphere-2023-2583
Preprint. Discussion started: 27 November 2023

ice-sheet models. There are a number of alternative subdivisions of the Antarctic continent, as for example in van der Linden et al. (2023), in which they differentiate between the Ross, Amundsen, Weddell, Peninsula, and an East Antarctic Ice Sheet ocean sector. In the Ross Sea however, they separate between the ocean in front of Victoria land (Drygalski region) and the rest of the Ross Sea. This makes their classification not suitable for our analysis, as we consider the continental-shelf break in front of Ross Sea representative for both regions.

When it comes to the effects of the potential warm water intrusion as analysed in our study, the difference between the critical temperatures is small in some cavities for physical reasons: this can be the case if the critical access depth of the basin is shallow and encompasses the colder surface waters, or if the current temperatures are already relatively warm, as in the case of the Amundsen region. While in some regions water masses reach the grounding lines rather gradually, there are also certain basins with an almost abrupt opening access to more than $g > 50$ % of the grounding line once a critical depth is transgressed (which we identify as prominent gateways). Evaluating critical temperatures and subsequent melt rates for a common circum-Antarctic threshold of $g = 50$ %, as we do in Fig. 2 and Fig. 5, may not capture the full impact that the basin's gateway may have (e.g. a prominent gateway providing $g = 30$ % grounding line access vs. one with $g = 60$ %). In some basins, warm water masses accessing $g = 30$ % of the region's grounding line could be sufficient to reach all fast flowing ice to cause significant ice loss, but in others $g > 50$ % is required. For those regions the most vulnerable parts of the grounding line may be located in shallower parts. Cavity geometries are highly heterogeneous and critical thresholds could thus be determined individually in a follow-up study taking into account other measures for the stability along the grounding line, e.g. buttressing, as in Naughten et al. (2023).

The temporal evolution of warm water accessing the Antarctic grounding lines at depth depends on the complex interplay of ice, ocean, atmosphere, and solid Earth. Importantly, the timing would mainly depend on the future climate change scenario determining the change in oceanic boundary conditions. We here aim at quantifying the potential effect this might have in the future. Ocean model projections show that warm water access under the Filchner–Ronne Ice Shelf may occur due to ongoing climate change, but that it is unlikely to happen within this century (Hellmer et al., 2012; Naughten et al., 2021; Haid et al., 2022). Other regions might also be susceptible to warm water intrusion: When assuming that sub-shelf melting becomes dominated by warm water intruding from the continental-shelf break, Jordan et al. (2023) find that the East Antarctic Ice Sheet might lose up to 48 mm of sea-level equivalent ice volume over the next 200 years. However, they artificially alter the ocean forcing to represent a shift to stronger on-shelf CDW transport.

5 Conclusion

In our study, we present a simple approach to calculate the access depths of water masses to Antarctic grounding lines. We combine latest available bathymetry data with ocean temperature and salinity observations. Thereby, we identify prominent oceanic gateways through which warm water masses residing off the continental-shelf break could potentially access the deep grounding lines in several Antarctic regions. Grounding lines positioned on retrograde, inland sloping topography are prone to the Marine Ice-Sheet instability (Weertman, 1974; Schoof, 2007; Reese et al., 2023, MISI). MISI can drive rapid retreat of

https://doi.org/10.5194/egusphere-2023-2583
Preprint. Discussion started: 27 November 2023

marine based ice (grounded below sea level), where sub-shelf melting leads to ice-shelf thinning, which in turn can lead to accelerated ice flow across the grounding line which can cause additional ice loss. Warm-water inflow to regions with deep-lying grounding lines and subsequent increased sub-shelf melting can thus have a strong impact on the ice flux across the grounding line and therefore the overall mass balance of the Antarctic Ice Sheet (Reese et al., 2018b; Goldberg et al., 2019).

Perturbing the current state of the Antarctic Ice Sheet with warmer temperatures at the continental-shelf break helps estimating an upper limit of melt rate changes. All regions would experience a strong increase in sub-shelf melting, while basal melt rates would shift by up to two orders of magnitudes in cavities that are currently in a 'cold' state. There, we estimate an increase in temperatures of around > 2°C.

While high resolution ocean modelling could provide a more detailed estimate on the effect of oceanic gateways on melting, our first-order approach is instead straight-forward and easy to run. The presented approach represents a refinement on identifying those ocean regions most relevant as input for PICO or other melt parameterisations. Identifying critical access depths could even inform geoengineering options such as proposed by Wolovick et al. (2023) that focus on the ocean access to dynamic (potentially driven by instabilities) glaciers in the Amundsen Sea. In their conceptual study, they investigate the potential of artificial barriers at critical access point to prevent further ice loss by sub-shelf melt.

To conclude, by identifying potential ocean gateways and analysing the thermal properties of ambient water masses, our study contributes to assessing the current and potential future vulnerability of the Antarctic Ice Sheet to changes in its surrounding ocean.

Code and data availability. The data and relevant code will be made publicly available on a public data repository i.e. PANGAEA or Zenodo. DOI links to the repositories will be provided upon publication.

https://doi.org/10.5194/egusphere-2023-2583
Preprint. Discussion started: 27 November 2023

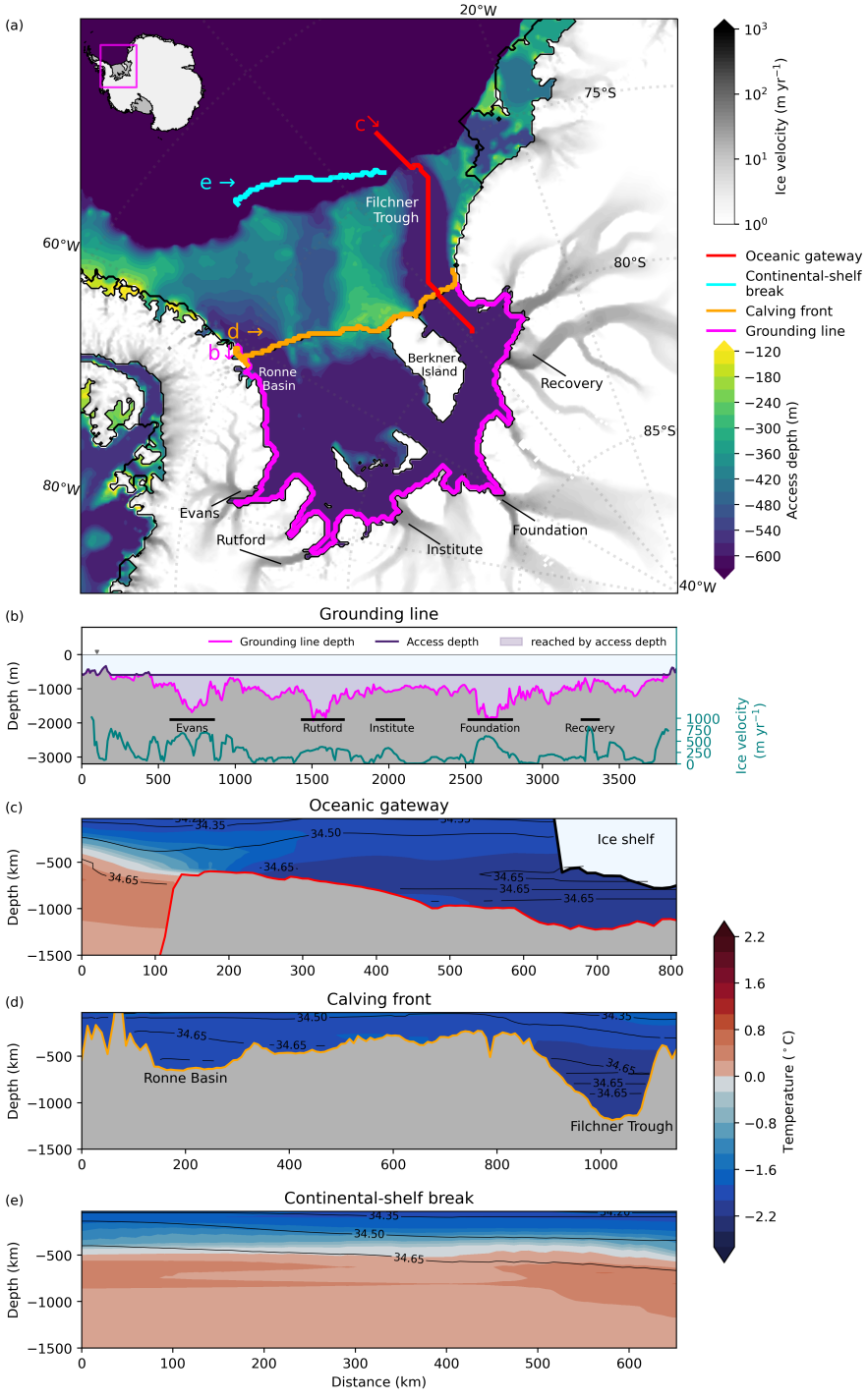

Figure 6. Access depths and temperature profiles for Filchner–Ronne Ice Shelf. (a) Computed access depths within the Weddell Sea indicate a prominent oceanic gateway along Filchner Trough towards Filchner–Ronne Ice Shelf. The transects denote vertical profiles along **(b)** the grounding line, **(c)** the oceanic gateway through Filchner Trough, **(d)** the calving front, and **(e)** the continental-shelf break. Speed of grounded ice in grey shading showing the location of major ice streams (in a) and as blue-green line (in b), taken from Mouginot et al. (2019). Magenta line (in b) indicates grounding line depth, while the dark purple line (in b) shows the derived access depth (e.g. d_c= -595 m).

https://doi.org/10.5194/egusphere-2023-2583
Preprint. Discussion started: 27 November 2023

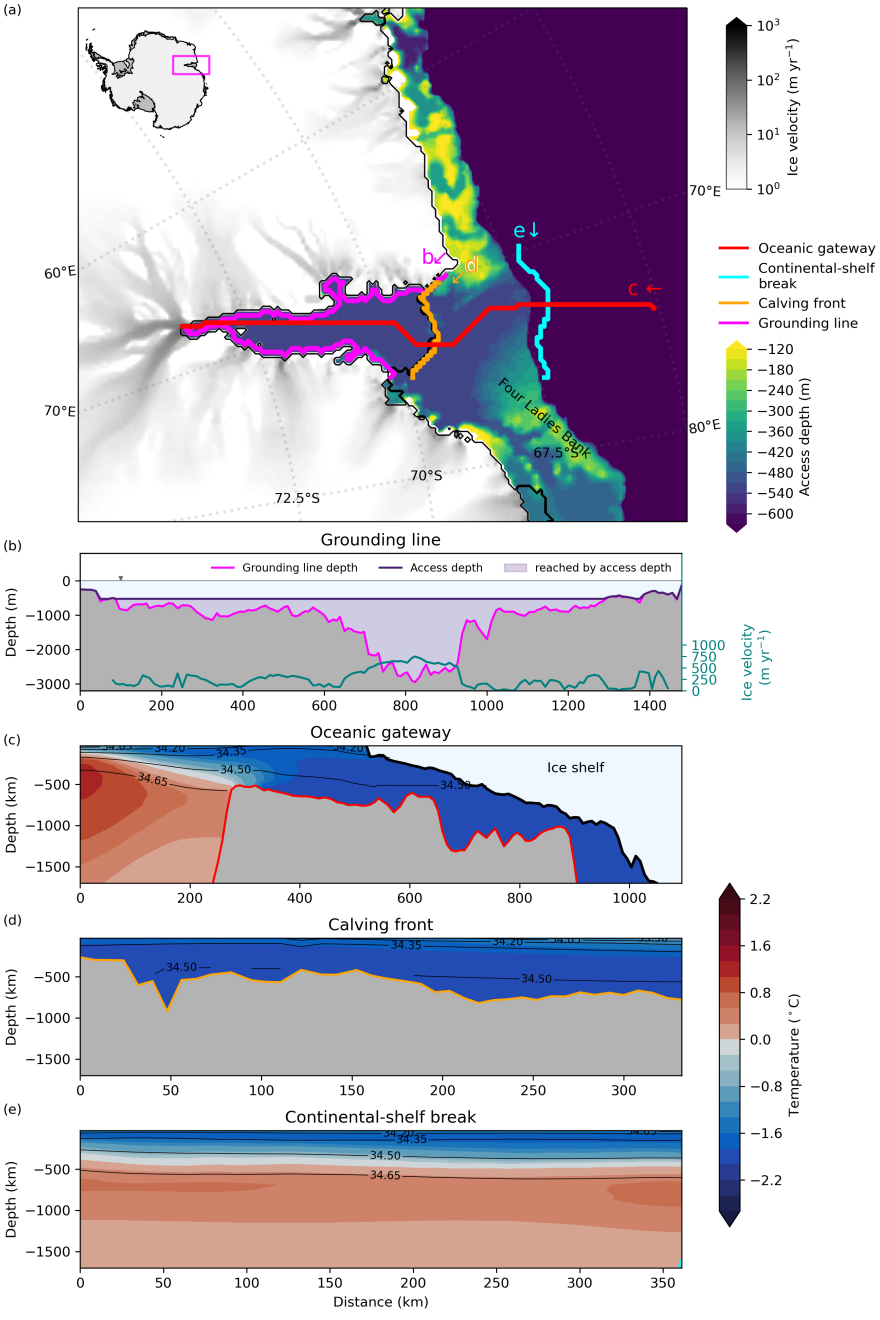

Figure 7. Access depths and temperature profiles for Amery Ice Shelf. (a) Computed access depths at Amery Ice Shelf indicate a prominent oceanic gateway along Prydz Channel. The transects denote vertical profiles along **(b)** the grounding line, **(c)** the oceanic gateway through Prydz Channel, **(d)** the calving front, and **(e)** the continental-shelf break. Speed of grounded ice in grey shading shows the location of major ice streams (in a) and as blue-green line (in b), taken from Mouginot et al. (2019). Magenta line (in b) indicates grounding line depth, while the dark purple line (in b) shows the derived access depth (e.g. d_c= -525 m).

https://doi.org/10.5194/egusphere-2023-2583
Preprint. Discussion started: 27 November 2023

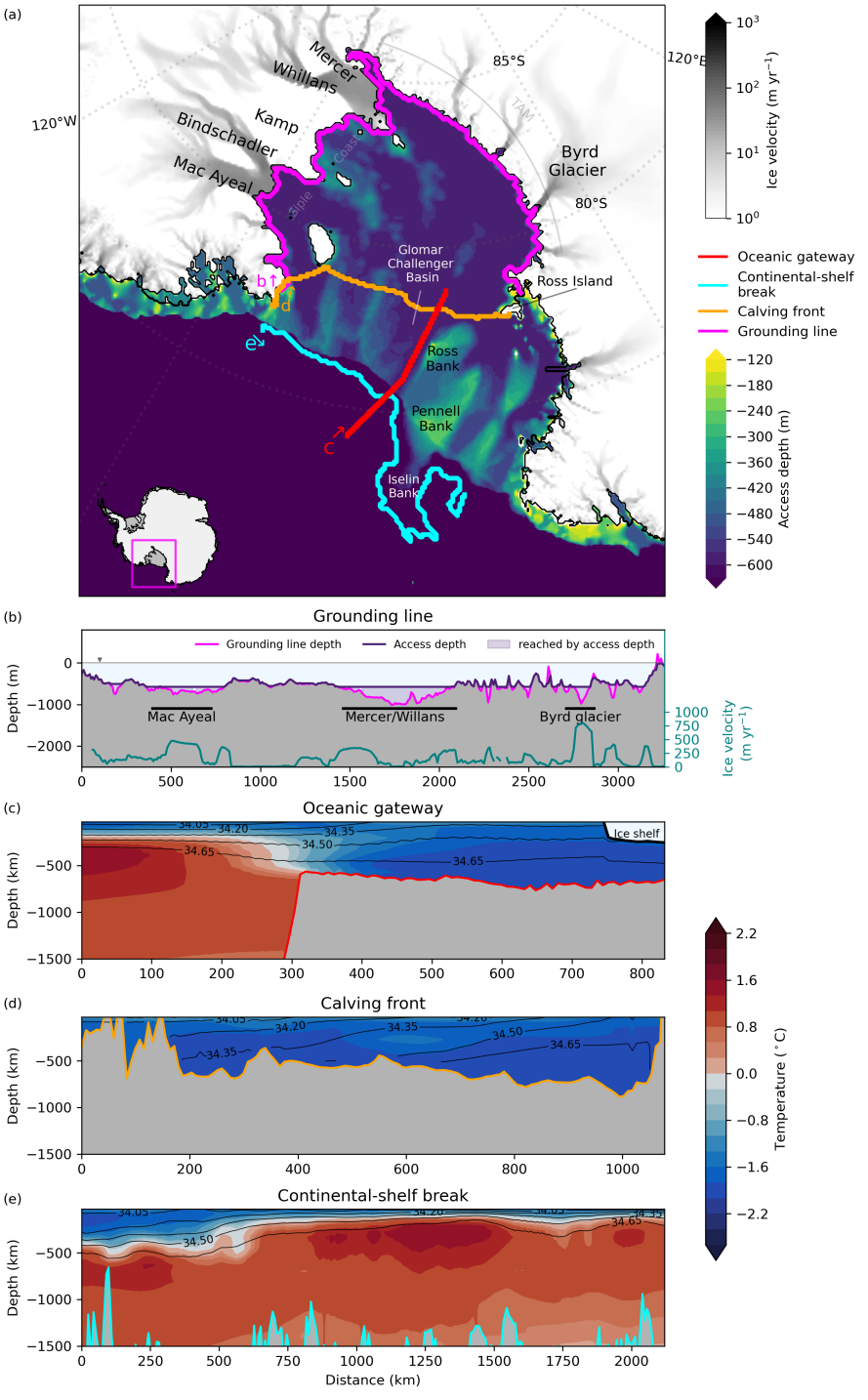

Figure 8. Access depths and temperature profiles for Ross Ice Shelf. (a) Computed access depths in the Ross Sea indicate a prominent oceanic gateway through Glomar Challenger Basin towards Ross Ice Shelf. The transects denote vertical profiles along **(b)** the grounding line, **(c)** the oceanic gateway through Glomar Challenger Basin, **(d)** the calving front, and **(e)** the continental-shelf break. Speed of grounded ice in grey shading shows the location of major ice streams (in a) and as blue-green line (in b), taken from Mouginot et al. (2019). Magenta line (in b) indicates grounding line depth, while the dark purple line (in b) shows the derived access depth (e.g. d_c= -570 m). TAM = Transantarctic Mountains.

https://doi.org/10.5194/egusphere-2023-2583
Preprint. Discussion started: 27 November 2023

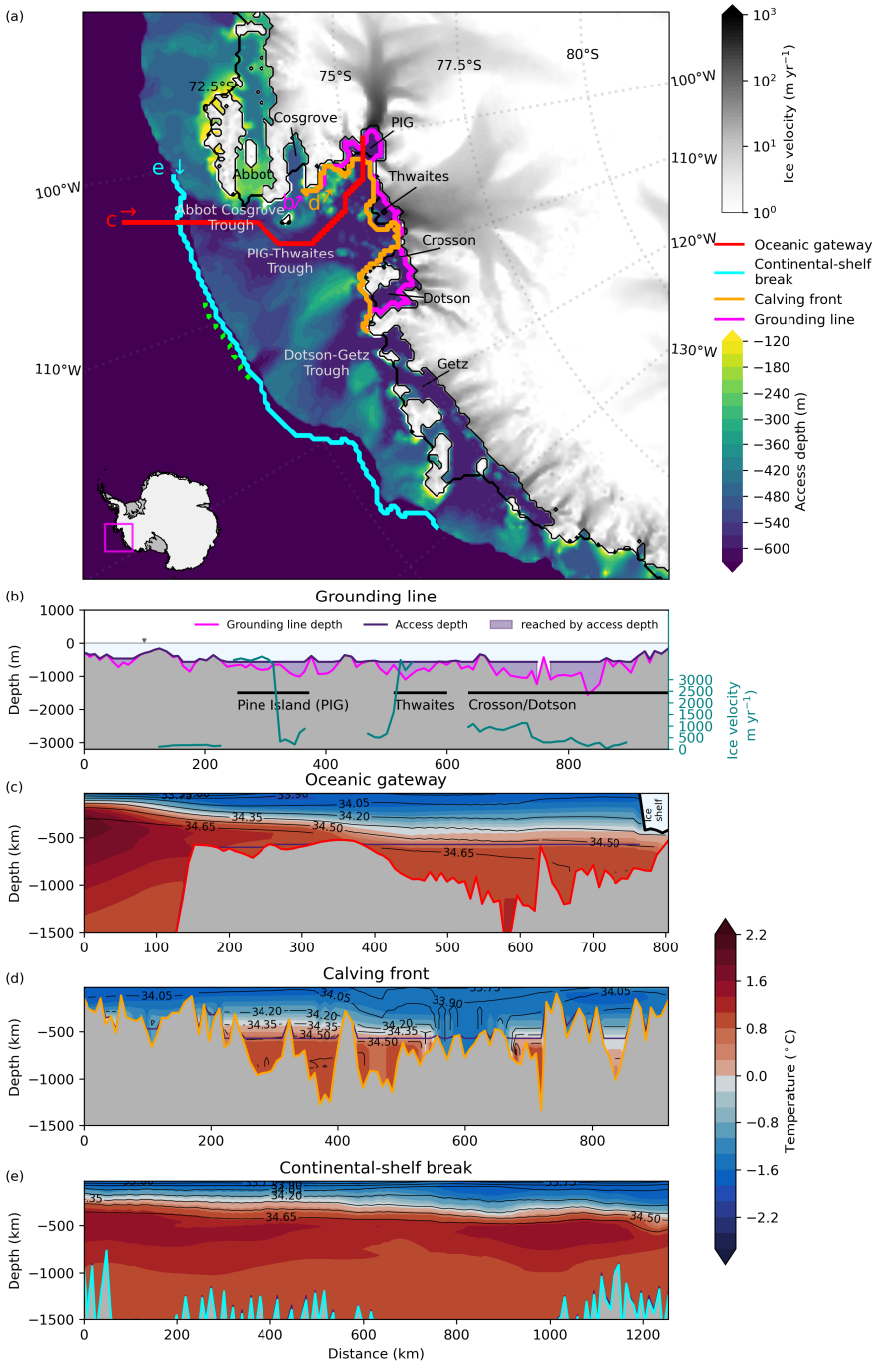

Figure 9. Access depths and temperature profiles in the Amundsen Sea region. (a) Computed access depths in the Amundsen Sea indicate a prominent oceanic gateway through Abbot Cosgrove Trough towards Pine Island and Thwaites glaciers. The transects denote vertical profiles along **(b)** the grounding line, **(c)** the oceanic gateway, **(d)** the calving front, and **(e)** the continental-shelf break. Speed of grounded ice in grey shading showing the location of major ice streams (in a) and as blue-green line (in b), taken from Mouginot et al. (2019). Magenta line (in b) indicates grounding line depth, while the dark purple line (in b) shows the derived access depth (e.g. d_c= -575 m). The part of the continental-shelf break (cyan) which is used to derived the critical temperature for the Amundsen basin (PICO basin 14) is indicated with green dots.

https://doi.org/10.5194/egusphere-2023-2583
Preprint. Discussion started: 27 November 2023

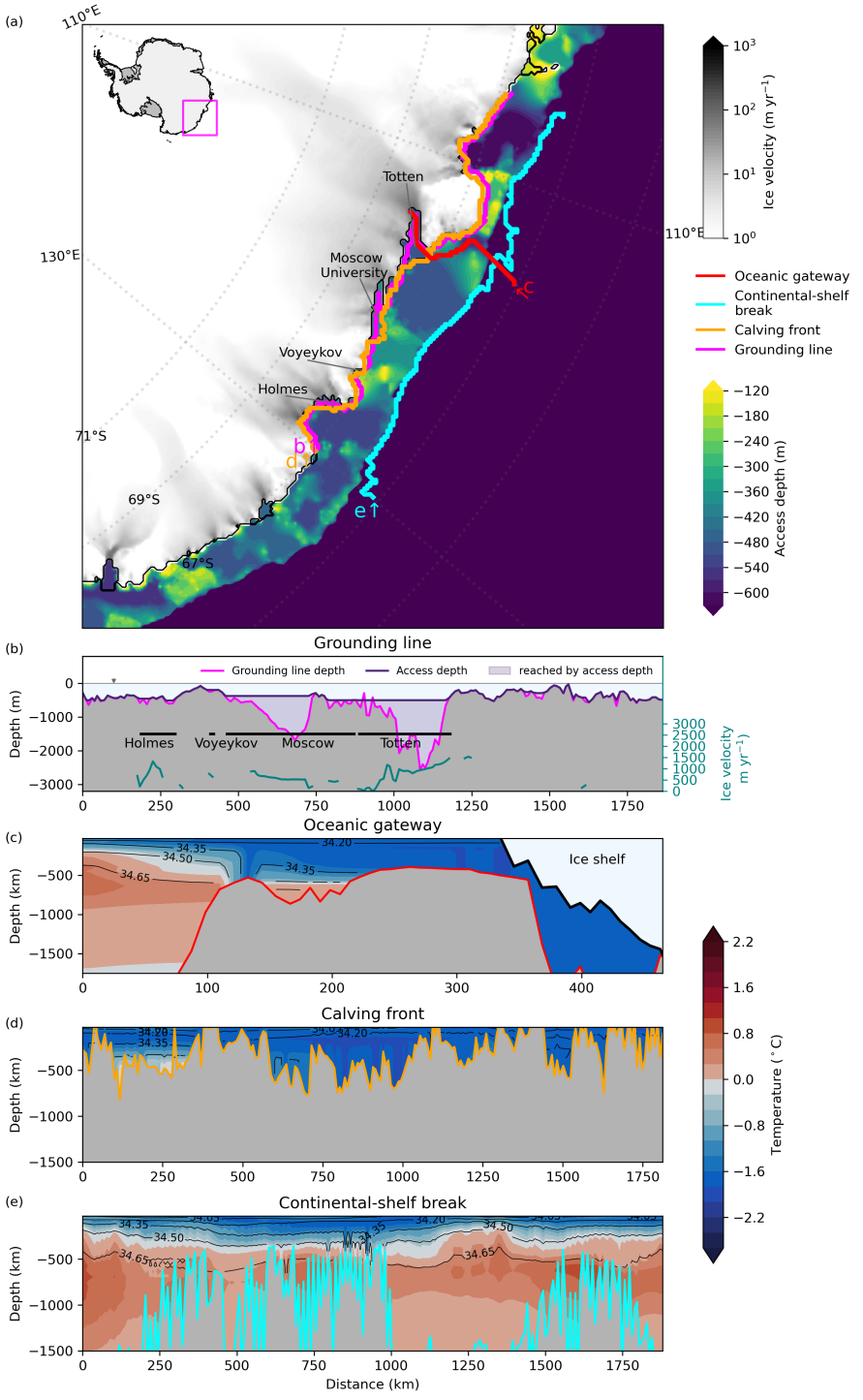

Figure A1. Access depths and temperature profiles in the Totten region, East Antarctica. (a) Computed access depths near Totten glacier indicate a prominent oceanic gateway near the Law Dome peninsula. The transects denote vertical profiles along **(b)** the grounding line, **(c)** the derived oceanic gateway, **(d)** the calving front, and **(e)** the continental-shelf break. Speed of grounded ice in grey shading showing the location of major ice streams (in a) and as blue-green line (in b), taken from Mouginot et al. (2019). Magenta line (in b) indicates grounding line depth, while the dark purple line (in b) shows the derived access depth (e.g. d_c= -495 m).

https://doi.org/10.5194/egusphere-2023-2583
Preprint. Discussion started: 27 November 2023

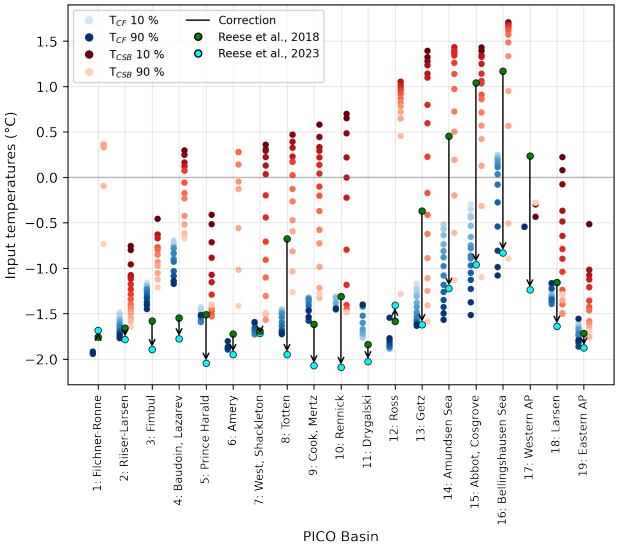

Figure A2. Comparison of critical temperatures with formerly used PICO input temperatures. Red and blue points show the critical temperatures determined in this study at the continental-shelf break, T_{CSB}, and calving front, T_{CF}, respectively. The extraction of these temperatures depend on the assumed grounding line access, which is determined from the flood-fill algorithm. Green markers depict the temperature input used in Reese et al. (2018a). The black line shows the temperature corrections applied for generating the input used in Reese et al. (2023) that are shown in cyan markers.

Author contributions. RW conceived the study and together with LN and RR designed the project. LN and RR performed initial analyses and proof of concept. LN made further analyses and together with MK, TA and RR refined the methodology. MK and TA performed the melt experiments. LN made the figures and, together with RR and RW drafted the manuscript, with strong support from all authors.

Competing interests. The authors declare that they have no conflict of interest.

Acknowledgements. LN was financially supported by a stipend from the Studienstiftung des Deutschen Volkes. LN, RR, MK and RW gratefully acknowledge support by the European Union's Horizon 2020 research and innovation programme under Grant Agreement No. 820575 (TiPACCs). RW further acknowledges support by the European Union's Horizon 2020 under Grant Agreement No. 869304 (PROTECT), by Deutsche Forschungsgemeinschaft (DFG) through grants WI4556/3-1 and WI4556/5-1. MK was financially supported by Deutsche Forschungsgemeinschaft (DFG) through grant WI4556/4-1 and the Potsdam Graduate School. TA and RW acknowledge funding by the PalMod project (FKZ: 01LP1925D, 01LP2305B), supported by the German Federal Ministry of Education and Research (BMBF) as a Research for Sustainability initiative (FONA). This work used resources of the Deutsches Klimarechenzentrum (DKRZ) granted by its Scientific Steering Committee (WLA) under project ID bk0993 (PalMod project). The authors gratefully acknowledge the European Regional Development Fund (ERDF), the German Federal Ministry of Education and Research and the Land Brandenburg for supporting this project

https://doi.org/10.5194/egusphere-2023-2583
Preprint. Discussion started: 27 November 2023

by providing resources on the high performance computer system at the Potsdam Institute for Climate Impact Research. Development of PISM is supported by NASA grants 20-CRYO2020-0052 and 80NSSC22K0274 and NSF grant OAC-2118285. The authors thank Ralph Timmermann and Hartmut Hellmer for fruitful discussions at an early stage of the project.

https://doi.org/10.5194/egusphere-2023-2583
Preprint. Discussion started: 27 November 2023

References

Adusumilli, S., Fricker, H. A., Medley, B., Padman, L., and Siegfried, M. R.: Interannual variations in meltwater input to the Southern Ocean from Antarctic ice shelves, Nature Geoscience, 13, 616–620, https://doi.org/10.1038/s41561-020-0616-z, 2020.

Alley, R. B., Anandakrishnan, S., Christianson, K., Horgan, H. J., Muto, A., Parizek, B. R., Pollard, D., and Walker, R. T.: Oceanic forcing of ice-sheet retreat: West Antarctica and more, Annual Review of Earth and Planetary Sciences, 43, 207–231, https://doi.org/10.1146/annurev-earth-060614-105344, 2015.

Arndt, J. E., Schenke, H. W., Jakobsson, M., Nitsche, F. O., Buys, G., Goleby, B., Rebesco, M., Bohoyo, F., Hong, J., Black, J., Greku, R., Udintsev, G., Barrios, F., Reynoso-Peralta, W., Taisei, M., and Wigley, R.: The International Bathymetric Chart of the Southern Ocean (IBCSO) Version 1.0—A new bathymetric compilation covering circum-Antarctic waters, Geophysical Research Letters, 40, 3111–3117, https://doi.org/https://doi.org/10.1002/grl.50413, 2013.

Assmann, K., Jenkins, A., Shoosmith, D., Walker, D., Jacobs, S., and Nicholls, K.: Variability of Circumpolar Deep Water transport onto the Amundsen Sea continental shelf through a shelf break trough, Journal of Geophysical Research: Oceans, 118, 6603–6620, https://doi.org/10.1002/2013JC008871, 2013.

Bart, P. J.: West-directed flow of the West Antarctic Ice Sheet across eastern basin, Ross Sea during the Quaternary, Earth and Planetary Science Letters, 228, 425–438, https://doi.org/10.1016/j.epsl.2004.10.014, 2004.

Bueler, E. and Brown, J.: Shallow shelf approximation as a "sliding law" in a thermomechanically coupled ice sheet model, Journal of Geophysical Research: Earth Surface, 114, https://doi.org/10.1029/2008JF001179, 2009.

Burgard, C., Jourdain, N. C., Reese, R., Jenkins, A., and Mathiot, P.: An assessment of basal melt parameterisations for Antarctic ice shelves, The Cryosphere, 16, 4931–4975, https://doi.org/10.5194/tc-16-4931-2022, 2022.

Daae, K., Hattermann, T., Darelius, E., Mueller, R. D., Naughten, K. A., Timmermann, R., and Hellmer, H. H.: Necessary conditions for warm inflow toward the Filchner Ice Shelf, Weddell Sea, Geophysical Research Letters, 47, e2020GL089 237, https://doi.org/10.1029/2020GL089237, 2020.

Darelius, E., Daae, K., Dundas, V., Fer, I., Hellmer, H. H., Janout, M., Nicholls, K. W., Sallée, J.-b., and Østerhus, S.: Observational evidence for on-shelf heat transport driven by dense water export in the Weddell Sea, Nature Communications, https://doi.org/10.1038/s41467-023-36580-3, 2023.

De Rydt, J., Holland, P. R., Dutrieux, P., and Jenkins, A.: Geometric and oceanographic controls on melting beneath Pine Island Glacier, Journal of Geophysical Research: Oceans, 119, 2420–2438, https://doi.org/10.1002/2013JC009513, 2014.

Drijfhout, S. S., Marshall, D. P., and Dijkstra, H. A.: Conceptual models of the wind-driven and thermohaline circulation, in: International Geophysics, vol. 103, pp. 257–282, Elsevier, https://doi.org/10.1016/B978-0-12-391851-2.00011-8, 2013.

Dutrieux, P., De Rydt, J., Jenkins, A., Holland, P. R., Ha, H. K., Lee, S. H., Steig, E. J., Ding, Q., Abrahamsen, E. P., and Schröder, M.: Strong sensitivity of Pine Island ice-shelf melting to climatic variability, Science, 343, 174–178, https://doi.org/10.1126/science.1244341, 2014.

Favier, L., Jourdain, N. C., Jenkins, A., Merino, N., Durand, G., Gagliardini, O., Gillet-Chaulet, F., and Mathiot, P.: Assessment of sub-shelf melting parameterisations using the ocean–ice-sheet coupled model NEMO (v3. 6)–Elmer/Ice (v8. 3), Geoscientific Model Development, 12, 2255–2283, 2019.

Flament, T. and Rémy, F.: Dynamic thinning of Antarctic glaciers from along-track repeat radar altimetry, Journal of Glaciology, 58, 830–840, https://doi.org/10.3189/2012JoG11J118, 2012.

https://doi.org/10.5194/egusphere-2023-2583
Preprint. Discussion started: 27 November 2023

Fricker, H. A., Warner, R. C., and Allison, I.: Mass balance of the Lambert Glacier–Amery Ice Shelf system, East Antarctica: a comparison of computed balance fluxes and measured fluxes, Journal of Glaciology, 46, 561–570, https://doi.org/10.3189/172756500781832765, 2000.

Goldberg, D. N., Gourmelen, N., Kimura, S., Millan, R., and Snow, K.: How Accurately Should We Model Ice Shelf Melt Rates?, Geophysical Research Letters, 46, 189–199, https://doi.org/10.1029/2018GL080383, 2019.

Gómez-Valdivia, F., Holland, P. R., Siahaan, A., Dutrieux, P., and Young, E.: Projected West Antarctic ocean warming caused by an expansion of the Ross Gyre, Geophysical Research Letters, 50, e2023GL102 978, https://doi.org/10.1029/2023GL102978, 2023.

Greenbaum, J., Blankenship, D., Young, D., Richter, T., Roberts, J., Aitken, A., Legresy, B., Schroeder, D., Warner, R., Van Ommen, T., et al.: Ocean access to a cavity beneath Totten Glacier in East Antarctica, Nature Geoscience, 8, 294, https://doi.org/10.1038/ngeo238, 2015.

Greene, C. A., Gardner, A. S., Schlegel, N.-J., and Fraser, A. D.: Antarctic calving loss rivals ice-shelf thinning, Nature, 609, 948–953, https://doi.org/10.1038/s41586-022-05037-w, 2022.

Gudmundsson, G. H., Paolo, F. S., Adusumilli, S., and Fricker, H. A.: Instantaneous Antarctic ice sheet mass loss driven by thinning ice shelves, Geophysical Research Letters, 46, 13 903–13 909, https://doi.org/10.1029/2019GL085027, 2019.

Haid, V., Timmermann, R., Gürses, Ö., and Hellmer, H. H.: On the drivers of regime shifts in the Antarctic marginal seas, EGUsphere, pp. 1–18, https://doi.org/10.5194/egusphere-2022-1044, 2022.

Haigh, M., Holland, P. R., and Jenkins, A.: The influence of bathymetry over heat transport onto the Amundsen Sea continental shelf, Journal of Geophysical Research: Oceans, p. e2022JC019460, https://doi.org/10.1029/2022JC019460, 2023.

Hattermann, T.: Antarctic thermocline dynamics along a narrow shelf with easterly winds, Journal of Physical Oceanography, 48, 2419–2443, https://doi.org/10.1175/JPO-D-18-0064.1, 2018.

Hein, A. S., Fogwill, C. J., Sugden, D. E., and Xu, S.: Glacial/interglacial ice-stream stability in the Weddell Sea embayment, Antarctica, Earth and Planetary Science Letters, 307, 211–221, https://doi.org/10.1016/j.epsl.2011.04.037, 2011.

Hellmer, H. H., Kauker, F., Timmermann, R., Determann, J., and Rae, J.: Twenty-first-century warming of a large Antarctic ice-shelf cavity by a redirected coastal current, Nature, 485, 225, https://doi.org/10.1038/nature11064, 2012.

Hellmer, H. H., Kauker, F., Timmermann, R., and Hattermann, T.: The Fate of the Southern Weddell Sea Continental Shelf in a Warming Climate, Journal of Climate, 30, 4337–4350, https://doi.org/10.1175/JCLI-D-16-0420.1, 2017.

Herraiz-Borreguero, L. and Naveira Garabato, A. C.: Poleward shift of Circumpolar Deep Water threatens the East Antarctic Ice Sheet, Nature Climate Change, 12, 728–734, https://doi.org/10.1038/s41558-022-01424-3, 2022.

Herraiz-Borreguero, L., Coleman, R., Allison, I., Rintoul, S. R., Craven, M., and Williams, G. D.: Circulation of modified C ircumpolar D eep W ater and basal melt beneath the A mery I ce S helf, E ast A ntarctica, Journal of Geophysical Research: Oceans, 120, 3098–3112, https://doi.org/10.1002/2015JC010697, 2015.

Heywood, K. J., Schmidtko, S., Heuzé, C., Kaiser, J., Jickells, T. D., Queste, B. Y., Stevens, D. P., Wadley, M., Thompson, A. F., Fielding, S., et al.: Ocean processes at the Antarctic continental slope, Philosophical Transactions of the Royal Society A: Mathematical, Physical and Engineering Sciences, 372, 20130 047, https://doi.org/10.1098/rsta.2013.0047, 2014.

Hirano, D., Tamura, T., Kusahara, K., Fujii, M., Yamazaki, K., Nakayama, Y., Ono, K., Itaki, T., Aoyama, Y., Simizu, D., et al.: On-shelf circulation of warm water toward the Totten Ice Shelf in East Antarctica, Nature Communications, 14, 4955, https://doi.org/10.1038/s41467-023-39764-z, 2023.

Hochmuth, K. and Gohl, K.: Glaciomarine sedimentation dynamics of the Abbot glacial trough of the Amundsen Sea Embayment shelf, West Antarctica, Geological Society, London, Special Publications, 381, 233–244, https://doi.org/10.1144/SP381.21, 2013.

https://doi.org/10.5194/egusphere-2023-2583
Preprint. Discussion started: 27 November 2023

Holland, D. M., Nicholls, K. W., and Basinski, A.: The Southern Ocean and its interaction with the Antarctic Ice Sheet, Science, 367, 1326–1330, https://doi.org/10.1126/science.aaz5491, 2020.

Holland, P. R., O'Connor, G. K., Bracegirdle, T. J., Dutrieux, P., Naughten, K. A., Steig, E. J., Schneider, D. P., Jenkins, A., and Smith, J. A.: Anthropogenic and internal drivers of wind changes over the Amundsen Sea, West Antarctica, during the 20th and 21st centuries, The Cryosphere, 16, 5085–5105, https://doi.org/10.5194/tc-16-5085-2022, 2022.

Jacobs, S., Helmer, H., Doake, C., Jenkins, A., and Frolich, R.: Melting of ice shelves and the mass balance of Antarctica, Journal of Glaciology, 38, 375–387, https://doi.org/10.3189/S0022143000002252, 1992.

Janout, M. A., Hellmer, H. H., Hattermann, T., Huhn, O., Sültenfuss, J., Østerhus, S., Stulic, L., Ryan, S., Schröder, M., and Kanzow, T.: FRIS revisited in 2018: On the circulation and water masses at the Filchner and Ronne Ice Shelves in the southern Weddell Sea, Journal of Geophysical Research: Oceans, 126, e2021JC017 269, https://doi.org/10.1029/2021JC017269, 2021.

Jenkins, A., Dutrieux, P., Jacobs, S., Steig, E. J., Gudmundsson, G. H., Smith, J., and Heywood, K. J.: Decadal ocean forcing and Antarctic ice sheet response: Lessons from the Amundsen Sea, Oceanography, 29, 106–117, https://www.jstor.org/stable/24862286, 2016.

Jenkins, A., Shoosmith, D., Dutrieux, P., Jacobs, S., Kim, T. W., Lee, S. H., Ha, H. K., and Stammerjohn, S.: West Antarctic Ice Sheet retreat in the Amundsen Sea driven by decadal oceanic variability, Nature Geoscience, 11, 733–738, https://doi.org/10.1038/s41561-018-0207-4, 2018.

Jordan, J. R., Miles, B., Gudmundsson, G., Jamieson, S., Jenkins, A., and Stokes, C.: Increased warm water intrusions could cause mass loss in East Antarctica during the next 200 years, Nature Communications, 14, 1825, https://doi.org/10.1038/s41467-023-37553-2, 2023.

Joughin, I., Alley, R. B., and Holland, D. M.: Ice-sheet response to oceanic forcing, Science, 338, 1172–1176, https://doi.org/10.1126/science.1226481, 2012.

Jourdain, N. C., Asay-Davis, X., Hattermann, T., Straneo, F., Seroussi, H., Little, C. M., and Nowicki, S.: A protocol for calculating basal melt rates in the ISMIP6 Antarctic ice sheet projections, The Cryosphere, https://doi.org/10.5194/tc-14-3111-2020, 2020.

Kenneally, J. P. and Hughes, T. J.: Basal melting along the floating part of Byrd Glacier, Antarctic Science, 16, 355–358, https://doi.org/10.1017/S0954102004002068, 2004.

Khudeev, R.: A new flood-fill algorithm for closed contour, in: 2005 Siberian Conference on Control and Communications, pp. 172–176, IEEE, https://doi.org/10.1109/SIBCON.2005.1611214, 2005.

Klages, J. P., Kuhn, G., Graham, A. G., Hillenbrand, C.-D., Smith, J., Nitsche, F. O., Larter, R. D., and Gohl, K.: Palaeo-ice stream pathways and retreat style in the easternmost Amundsen Sea Embayment, West Antarctica, revealed by combined multibeam bathymetric and seismic data, Geomorphology, 245, 207–222, https://doi.org/10.1016/j.geomorph.2015.05.020, 2015.

Kreuzer, M., Albrecht, T., Nicola, L., and Winkelmann, R.: Oceanic gateways in Antarctica - Part B: Impact of relative sea-level change on sub-shelf melt, in prep., 2023.

Kumar, B., Tiwari, U. K., Kumar, S., Tomer, V., and Kalra, J.: Comparison and performance evaluation of boundary fill and flood fill algorithm, Int. J. Innov. Technol. Explor. Eng, 8, 9–13, https://doi.org/10.35940/ijitee.L1002.10812S319, 2020.

Larter, R. D., Graham, A. G., Hillenbrand, C.-D., Smith, J. A., and Gales, J. A.: Late Quaternary grounded ice extent in the Filchner Trough, Weddell Sea, Antarctica: new marine geophysical evidence, Quaternary Science Reviews, 53, 111–122, https://doi.org/10.1016/j.quascirev.2012.08.006, 2012.

Law, G.: Quantitative comparison of flood fill and modified flood fill algorithms, International Journal of Computer Theory and Engineering, 5, 503–508, https://doi.org/10.7763/IJCTE.2013.V5.738, 2013.

https://doi.org/10.5194/egusphere-2023-2583
Preprint. Discussion started: 27 November 2023

Lewis, E. L. and Perkin, R. G.: Ice pumps and their rates, Journal of Geophysical Research: Oceans, 91, 11 756–11 762, https://doi.org/10.1029/JC091iC10p11756, 1986.

Li, T., Dawson, G. J., Chuter, S. J., and Bamber, J. L.: Grounding line retreat and tide-modulated ocean channels at Moscow University and Totten Glacier ice shelves, East Antarctica, The Cryosphere, 17, 1003–1022, https://doi.org/10.5194/tc-17-1003-2023, 2023.

Mackintosh, A. N., Verleyen, E., O'Brien, P. E., White, D. A., Jones, R. S., McKay, R., Dunbar, R., Gore, D. B., Fink, D., Post, A. L., et al.: Retreat history of the East Antarctic Ice Sheet since the last glacial maximum, Quaternary Science Reviews, 100, 10–30, https://doi.org/10.1016/j.quascirev.2013.07.024, 2014.

Millan, R., Rignot, E., Bernier, V., Morlighem, M., and Dutrieux, P.: Bathymetry of the Amundsen Sea Embayment sector of West Antarctica from Operation IceBridge gravity and other data, Geophysical Research Letters, 44, 1360–1368, https://doi.org/10.1002/2016GL072071, 2017.

Morlighem, M.: MEaSUREs BedMachine Antarctica, Version 3, https://doi.org/10.5067/FPSU0V1MWUB6, [Dataset], accessed 1 July 2022, 2022.

Morlighem, M., Rignot, E., Binder, T., Blankenship, D., Drews, R., Eagles, G., Eisen, O., Ferraccioli, F., Forsberg, R., Fretwell, P., et al.: Deep glacial troughs and stabilizing ridges unveiled beneath the margins of the Antarctic ice sheet, Nature Geoscience, 13, 132–137, https://doi.org/10.1038/s41561-019-0510-8, 2020.

Mouginot, J., Rignot, E., and Scheuchl, B.: Sustained increase in ice discharge from the Amundsen Sea Embayment, West Antarctica, from 1973 to 2013, Geophysical Research Letters, 41, 1576–1584, https://doi.org/10.1002/2013GL059069, 2014.

Mouginot, J., Rignot, E., and Scheuchl, B.: Continent-wide, interferometric SAR phase, mapping of Antarctic ice velocity, Geophysical Research Letters, 46, 9710–9718, https://doi.org/10.1029/2019GL083826, 2019.

Mueller, R. D., Hattermann, T., Howard, S. L., and Padman, L.: Tidal influences on a future evolution of the Filchner–Ronne Ice Shelf cavity in the Weddell Sea, Antarctica, The Cryosphere, 12, 453–476, https://doi.org/10.5194/tc-12-453-2018, 2018.

Naughten, K. A., De Rydt, J., Rosier, S. H., Jenkins, A., Holland, P. R., and Ridley, J. K.: Two-timescale response of a large Antarctic ice shelf to climate change, Nature Communications, 12, 1991, https://doi.org/10.1038/s41467-021-22259-, 2021.

Naughten, K. A., Holland, P. R., and De Rydt, J.: Unavoidable future increase in West Antarctic ice-shelf melting over the twenty-first century, Nature Climate Change, https://doi.org/10.1038/s41558-023-01818-x, 2023.

Nicholls, K. W., Østerhus, S., Makinson, K., Gammelsrød, T., and Fahrbach, E.: Ice-ocean processes over the continental shelf of the southern Weddell Sea, Antarctica: A review, Reviews of Geophysics, 47, https://doi.org/10.1029/2007RG000250, 2009.

Nitsche, F. O., Jacobs, S. S., Larter, R. D., and Gohl, K.: Bathymetry of the Amundsen Sea continental shelf: Implications for geology, oceanography, and glaciology, Geochemistry, Geophysics, Geosystems, 8, https://doi.org/https://doi.org/10.1029/2007GC001694, 2007.

Olbers, D. and Hellmer, H.: A box model of circulation and melting in ice shelf caverns, Ocean Dynamics, 60, 141–153, https://doi.org/10.1007/s10236-009-0252-z, 2010.

Owolana, B.: Evaluating the duration of post-LGM grounding events in the Glomar Challenger Basin paleotrough, Eastern Basin Antarctica, using sediment flux calculations, Louisiana State University and Agricultural & Mechanical College, https://doi.org/10.31390/gradschool_theses.3209, 2011.

Paolo, F. S., Fricker, H. A., and Padman, L.: Volume loss from Antarctic ice shelves is accelerating, Science, 348, 327–331, https://doi.org/10.1126/science.aaa0940, 2015.

Pritchard, H., Ligtenberg, S., Fricker, H., Vaughan, D., Van den Broeke, M., and Padman, L.: Antarctic ice-sheet loss driven by basal melting of ice shelves, Nature, 484, 502, https://doi.org/10.1038/nature10968, 2012.

https://doi.org/10.5194/egusphere-2023-2583
Preprint. Discussion started: 27 November 2023

Pritchard, H. D., Arthern, R. J., Vaughan, D. G., and Edwards, L. A.: Extensive dynamic thinning on the margins of the Greenland and Antarctic ice sheets, Nature, 461, 971–975, https://doi.org/10.1038/nature08471, 2009.

Reese, R., Albrecht, T., Mengel, M., Asay-Davis, X., and Winkelmann, R.: Antarctic sub-shelf melt rates via PICO, The Cryosphere, 12, 1969–1985, https://doi.org/10.5194/tc-12-1969-2018, 2018a.

Reese, R., Gudmundsson, G. H., Levermann, A., and Winkelmann, R.: The far reach of ice-shelf thinning in Antarctica, Nature Climate Change, 8, 53, https://doi.org/10.1038/s41558-017-0020-x, 2018b.

Reese, R., Garbe, J., Hill, E. A., Urruty, B., Naughten, K. A., Gagliardini, O., Durand, G., Gillet-Chaulet, F., Gudmundsson, G. H., Chandler, D., Langebroek, P. M., and Winkelmann, R.: The stability of present-day Antarctic grounding lines – Part 2: Onset of irreversible retreat of Amundsen Sea glaciers under current climate on centennial timescales cannot be excluded, The Cryosphere, 17, 3761–3783, https://doi.org/10.5194/tc-17-3761-2023, 2023.

Rignot, E., Jacobs, S., Mouginot, J., and Scheuchl, B.: Ice-shelf melting around Antarctica, Science, 341, 266–270, https://doi.org/10.1126/science.1235798, 2013.

Schmidtko, S., Heywood, K. J., Thompson, A. F., and Aoki, S.: Multidecadal warming of Antarctic waters, Science, 346, 1227–1231, https://doi.org/10.1126/science.1256117, 2014.

Schoof, C.: Ice sheet grounding line dynamics: Steady states, stability, and hysteresis, Journal of Geophysical Research: Earth Surface, 112, https://doi.org/10.1029/2006JF000664, 2007.

Silvano, A., Rintoul, S. R., and Herraiz-Borreguero, L.: Ocean-ice shelf interaction in East Antarctica, Oceanography, 29, 130–143, http://www.jstor.org/stable/24862288, 2016.

Sun, C., Liu, C., Wang, Z., Yan, L., Tao, Y., Qin, Q., and Qian, J.: On the influences of the continental shelf bathymetry correction in Prydz Bay, East Antarctica, Frontiers in Marine Science, 9, 957 414, https://doi.org/10.3389/fmars.2022.957414, 2022.

Thoma, M., Jenkins, A., Holland, D., and Jacobs, S.: Modelling circumpolar deep water intrusions on the Amundsen Sea continental shelf, Antarctica, Geophysical Research Letters, 35, https://doi.org/10.1029/2008GL034939, 2008.

Tinto, K., Padman, L., Siddoway, C., Springer, S., Fricker, H., Das, I., Caratori Tontini, F., Porter, D., Frearson, N., Howard, S., et al.: Ross Ice Shelf response to climate driven by the tectonic imprint on seafloor bathymetry, Nature Geoscience, 12, 441–449, https://doi.org/10.1038/s41561-019-0370-2, 2019.

van der Linden, E. C., Le Bars, D., Lambert, E., and Drijfhout, S.: Antarctic contribution to future sea level from ice shelf basal melt as constrained by ice discharge observations, The Cryosphere, 17, 79–103, https://doi.org/10.5194/tc-17-79-2023, 2023.

Vaňková, I., Winberry, J. P., Cook, S., Nicholls, K. W., Greene, C. A., and Galton-Fenzi, B. K.: High spatial melt rate variability near the Totten Glacier grounding zone explained by new bathymetry inversion, Geophysical Research Letters, 50, e2023GL102 960, https://doi.org/10.1029/2023GL102960, 2023.

Walker, D. P., Brandon, M. A., Jenkins, A., Allen, J. T., Dowdeswell, J. A., and Evans, J.: Oceanic heat transport onto the Amundsen Sea shelf through a submarine glacial trough, Geophysical Research Letters, 34, https://doi.org/10.1029/2006GL028154, 2007.

Wang, Y., Zhou, M., Zhang, Z., and Dinniman, M. S.: Seasonal variations in Circumpolar Deep Water intrusions into the Ross Sea continental shelf, Frontiers in Marine Science, 10, https://doi.org/10.3389/fmars.2023.1020791, 2023.

Weertman, J.: Stability of the junction of an ice sheet and an ice shelf, Journal of Glaciology, 13, 3–11, https://doi.org/10.3189/S0022143000023327, 1974.

https://doi.org/10.5194/egusphere-2023-2583
Preprint. Discussion started: 27 November 2023

Williams, G. D., Herraiz-Borreguero, L., Roquet, F., Tamura, T., Ohshima, K. I., Fukamachi, Y., Fraser, A. D., Gao, L., Chen, H., McMahon, C. R., Harcourt, R., and Hindell, M.: The suppression of Antarctic bottom water formation by melting ice shelves in Prydz Bay, Nature Communications, 7, 12 577, https://doi.org/10.1038/ncomms12577, 2016.

Winkelmann, R., Martin, M. A., Haseloff, M., Albrecht, T., Bueler, E., Khroulev, C., and Levermann, A.: The Potsdam parallel ice sheet model (PISM-PIK)–Part 1: Model description, The Cryosphere, 5, 715–726, https://doi.org/10.5194/tc-5-715-2011, 2011.

Wolovick, M., Moore, J., and Keefer, B.: The potential for stabilizing Amundsen Sea glaciers via underwater curtains, PNAS nexus, 2, pgad103, https://doi.org/10.1093/pnasnexus/pgad103, 2023.

Wouters, B., Martin-Español, A., Helm, V., Flament, T., van Wessem, J. M., Ligtenberg, S. R., Van den Broeke, M. R., and Bamber, J. L.: Dynamic thinning of glaciers on the Southern Antarctic Peninsula, Science, 348, 899–903, https://doi.org/10.1126/science.aaa5727, 2015.

Zwally, H. J., Giovinetto, M. B., Beckley, M. A., and Saba, J. L.: Antarctic and Greenland Drainage Systems, http://imbie.org/imbie-3/drainage-basins/, [Dataset], accessed 27 November 2018, 2012.